Small Linear Antennas

by

Mohammod Ali

Bachelor of Science in Engineering (Electrical & Electronic), Bangladesh
University of Engineering & Technology, Dhaka, 1987

A Thesis Submitted in Partial Fulfillment of the
Requirements for the Degree of

MASTER OF APPLIED SCIENCE

in the Department of Electrical & Computer Engineering

We accept this thesis as conforming
to the required standard

[redacted]

Dr. S. S. Stuchly, Supervisor, Dept. of Elec. & Comp. Eng.

[redacted]

Dr. J. Bornemann, Departmental Member, Dept. of Elec. & Comp. Eng.

[redacted]

Dr. D. Olesky, Outside Member, Dept. of Comp. Science

[redacted]

Dr. R. H. Johnston, External Examiner, Dept. of Elec. & Comp. Eng.,
University of Calgary

Supervisor: Dr. S. S. Stuchly

Abstract

The input impedance and the bandwidth, two important characteristics of bent linear antennas, e.g. the meander, the sinusoidal and the dual meander have been investigated while developing small wideband antennas for application in personal communication network (PCN) [1]-[3] handsets operating around 880 MHz and 1900 MHz. Bandwidth characteristics of several sleeve antenna configurations have also been investigated to develop an antenna which would operate in both the PCN bands. Since a variety of antenna configurations were considered, and since no single numerical model was available for all the configurations, experimental methods were chosen as the appropriate means of investigation.

In the course of experimental analysis a number of sinusoidal and meander antennas were measured and their bandwidths and shortening ratios were correlated with the design variables. The results found for the sinusoidal antenna can be used as a guideline by a designer who is interested in a specific shortening ratio but is uncertain about its bandwidth restriction. It has been found that for the same shortening ratio the sinusoidal antenna has better VSWR frequency characteristics than the meander. Specifically for PCN handset applications several bent antennas have been developed. Finally, a new explanation of the phenomenon of shortening of bent antennas has been proposed.

Examiners:

[redacted]

Dr. S. S. Stuchly, Supervisor, Dept. of Elec. & Comp. Eng.

[redacted]

Dr. J. Bornemann, Departmental Member, Dept. of Elec. & Comp. Eng.

[redacted]

Dr. D. Olesky, Outside Member, Dept. of Comp. Science

[redacted]

Dr. R. H. Johnston, External Examiner, Dept. of Elec. & Comp. Eng.,

University of Calgary

Contents

List of Figures

List of Tables

Acknowledgements

I wish to express my deepest gratitude to my supervisor, Dr. S. S. Stuchly for his continuous encouragement and guidance shown throughout this research work and the process of writing this manuscript.

I would like to acknowledge the indebtedness to my colleague, Krzysztof Caputa for his day to day help in arranging the experimental setup and performing measurements. A hearty thank is also extended to all colleagues in the department from whom I received valuable suggestions and help.

Finally, I express my gratitude to my wife, my son and my daughter for enduring the lonely moments and for providing me with the energy and enthusiasm needed to accomplish this work.

To The Memory of My Loving Father

Chapter 1

Introduction

1.1 Motivation

Linear antennas are one of the oldest and still the most prevalent of all antenna types below a few GHz. They are simple, easy to make, and inexpensive. Because of their versatility in many applications, they have been investigated extensively analytically, numerically and experimentally.

The growing demand from personal communication [1]-[3] industry calls for small, wideband antennas. These antennas would operate as PCN (personal communication network) handset antennas around 880 MHz [4] and 1900 MHz [5]. A small, simple, compact and lightweight antenna with good radiation characteristics, would be of great advantage to the portable telephone user.

The term 'Small Antenna' is used to describe antennas which are electrically small. Wheeler[6] defines a small antenna as an antenna occupying a small fraction of one radiansphere ($\frac{\lambda}{2\pi}$) , where λ is the wavelength corresponding to the design frequency. Typically the greatest dimension of a small antenna should be less than $\frac{1}{4}\lambda$ (including any image). According to this definition, an electrically small monopole will approximately be 4.26 cm long at 880 MHz and 1.97 cm long at 1900 MHz.

Unlike the VLF (3–30 kHz) and LF (30–300 kHz) antennas the frequency range of interest here ensures that if an antenna is electrically small then it would also be small physically. However, an electrically small antenna acts largely either as a capacitor or an inductor depending upon whether it is a small dipole or a small loop [6]. The capacitive behavior of a small dipole can be proved by applying transmission line theory. Considering the antenna as a flared open-circuited transmission line, the input impedance at a distance l from the open end is [7]

$$Z_{in} = -jZ_o \cot \beta l \tag{1.1}$$

where Z_o is the characteristic impedance of the line, $\beta = \frac{2\pi}{\lambda}$, is the phase constant and l is the length of the line. Since any small dipole has a length, $l < \frac{\lambda}{4}$, Z_{in} according to (1.1) is always capacitive with some radiation resistance.

To get an idea about the input resistances of small antennas let us consider a small dipole. The input impedance of such an antenna of length l and wire radius a is given by [7]

$$Z_{in} = 20\pi^2(\frac{l}{\lambda})^2 - j120\frac{[\ln(\frac{l}{2a}) - 1]}{\tan(\pi\frac{l}{\lambda})}. \tag{1.2}$$

From (1.2), Z_{in} for a dipole of length 0.24λ and wire radius 0.001λ is $11.37 -$

$j483.99\Omega$. Although the input capacitive reactance in this case can be tuned to zero by adding an inductance, the antenna will still present a large mismatch when connected to practical transmission lines, many of which have characteristic impedances of 50 or 75Ω. Therefore, because of this impedance mismatch, most of the power fed to the antenna will be reflected and the VSWR of the antenna will be high. Similar will be the case with a small loop which is inherently inductive [8].

Therefore, instead of investigating electrically small antennas the approach here was to use the straight monopole configuration and to bend or otherwise modify it according to some specific geometric pattern to achieve the desired shortening effect. In the process of modification another important point was considered and that was how to achieve greater bandwidth without much compromise in polarization, gain, radiation pattern and efficiency.

The term 'bandwidth' is defined as the frequency range of operation of an antenna within a VSWR (voltage standing wave ratio) of $2:1$. Bandwidth is computed in either of two ways. Let f_U and f_L be the upper and the lower frequencies of operation of an antenna within a VSWR of $2:1$. Let us also assume that the center frequency of the antenna is f_C, then bandwidth can either be expressed as a percent of the center frequency or as a ratio of the upper and the lower frequency.

In equation form bandwidth when expressed as a percent of the center frequency is given by

$$\frac{f_U - f_L}{f_C} \times 100 \tag{1.3}$$

[8]. On the other hand bandwidth when expressed as a ratio of the upper and the

lower frequencies is given by

$$\frac{f_U}{f_L} \tag{1.4}$$

[8]. The bandwidth of narrowband antennas is usually expressed as a percent using (1.3) whereas that of wideband antennas is expressed as a ratio using (1.4) [8]. In this thesis the bandwidth of straight or bent monopole antennas is expressed as a percent and that of the sleeve antennas is expressed as a ratio.

1.2 Objective

The objective of this thesis was to investigate some possibilities of designing small, wideband antennas for use in personal communication network handsets. The term 'small' is used here to represent antennas which are both electrically and mechanically smaller than straight quarter-wave monopoles. The term 'wideband antenna' is used here to indicate an antenna which has a bandwidth greater than that of a thin dipole (length to diameter ratio, $\frac{l}{d} = 5000$ or higher). For example, a dipole with an $\frac{l}{d}$ of 5000 has a bandwidth of 3% [7].

To develop small antennas bent linear antenna configurations were considered. The configurations chosen for this purpose are: (a) *The meander*, Nakano *et al.* [9], (b) *The sinusoidal*, a new configuration proposed here which is similar to the zigzag, Nakano *et al.* [9], and (c) *The dual meander*, Wong *et al.* [10].

Since by bending an antenna its input impedance, bandwidth, radiation pattern, polarization, gain etc. changes [9]-[12], careful design procedures are necessary to obtain the desired antenna characteristics. It has been reported that within some

design limits (which will be discussed later in Chapter 3) the radiation pattern, polarization and gain of a bent antenna are identical to a straight quarter wave monopole [9]-[12]. But even within these limits the input impedance of any bent antenna has been found to be much different than a straight monopole [9].

Therefore, it is important that the variation of bandwidth which occurs due to the variation of input impedance be understood and correlated with the design variables of the antenna. By this way a designer can have an idea about how much bandwidth can be obtained from a short bent antenna. To accomplish this objective the sinusoidal and the meander configurations were considered and characteristics of a number of such antennas were investigated.

During this process efforts were made to determine the best possible design parameters so that small wideband antennas can be developed for PCN handset applications. To develop such antennas investigations were conducted on antennas in three categories:

1. Bent wire antennas: wires were bent to develop such antennas
2. Printed bent antennas: the configurations were etched on a dielectric substrate to achieve higher shortening than the bent wire antennas
3. Sleeve antennas: a broadband sleeve antenna was designed to develop a dual band antenna that can be used in both PCN bands

Because of the diversity of antenna types and also because of the complicated geometries, experimental methods were adopted as the tool of investigations.

1.3 Present State of Knowledge

Linear antennas were extensively studied by many researchers [13] - [37] throughout the past decades. Either theoretical or experimental methods or both were used. They formulated integral or integro-differential equations for such antennas and solved those equations numerically to determine different antenna characteristics like current distribution, input impedance, radiation pattern etc. Some of them derived simplified expressions for the input impedance of a cylindrical antenna [14].

Experimental methods were used for two specific reasons – (1) to validate the theoretical findings, and (2) to determine the radiation characteristics of an antenna when the antenna possesses complicated geometry making it difficult or impossible for analytical or numerical evalutaion of its characteristics.

An integrated approach was taken by King [13] to establish a bridge between the analytical and experimental results for linear antennas. Many curves, tables and design data along with detailed analytical and experimental methods have been presented.

With the advent of digital computers, linear antennas have been studied using the Method of Moments (MoM). For the cylindrical dipole this method uses the Hallen or the Pocklington type integral equation to determine the current distribution, input impedance, radiation pattern and other antenna characteristics. Monopole antennas on ground plane of infinite extension can be modelled as dipoles by applying the image theory. But configurations like a straight monopole on a small finite size ground plane can not be modelled as a dipole applying the image theory because of the diffraction from the edges of the ground plane. Therefore, for such antennas the

integral equation is to be derived first and then solved to determine its characteristics [19]. Derivation of integral equation is also necessary if the antenna is arbitrarily bent [37]. A very concise list of references dealing with the Method of Moments applied in linear antenna problems can be found in [15] - [23]. Application of FDTD (Finite Difference Time Domain) technique has also been reported [24].

Weiner *et al.* [25] presented a detailed review on monopole antennas along with their own contribution in this field. They analyzed a very thin monopole antenna on an infinite ground plane using the image theory and then derived simplified expressions for the input impedance of that antenna. Their treatment of the wire monopole antenna also includes a wire on a ground plane with zero radius. They summarized the state of the art in numerical models for straight wire monopole antennas on finite size ground planes. Useful results found from different numerical models were presented in tabular and in graphical forms in [25]. Those results were then compared with their own numerical and experimental results [25].

A detailed discussion of the characteristics of small antennas was presented by Wheeler [6]. We know that a small antenna has low radiation resistance. Low radiation resistance results in low radiation power factor which makes such antennas very inefficient. Because efficiency of small antennas is defined as [6]

$$e = \frac{RF}{RF + LF} \tag{1.5}$$

where RF is the radiation power factor and LF is the loss power factor. Also the bandwidth of such a small antenna would be limited by its radiation power factor. As an example he [6] described the largest antenna in the world which is an electrically small antenna. It works at a frequency of 15.5 kHz. The antenna has an effective height of 185 m and an effective area of 3.4 square kilometers. It has a

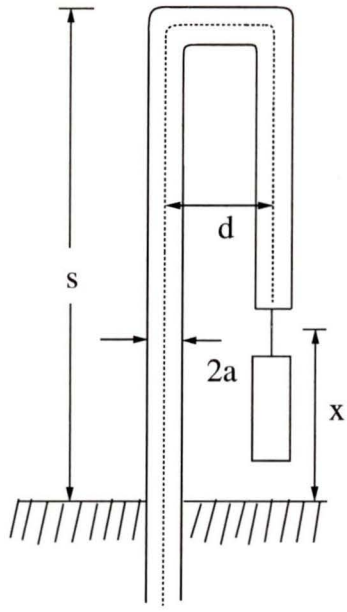

Figure 1.1: The open folded unipole antenna of Josephson [26]

radiation resistance of 0.144 Ω, input power of 2 MW and radiated power of 1 MW. Thus the antenna has an efficiency of 50%.

Josephson [26] presented an open folded unipole antenna with a displaced feed-point. The antenna is shown in Fig. 1.1 where $s = 0.15\lambda$, $d = 0.015\lambda$, $x = 0.0714\lambda$ and $2a = 0.0035\lambda$. It is a short bent sleeve monopole where the sleeve displaces the feed point and after the sleeve section the inner conductor is extended with increased diameter. The antenna operates at a center frequency of 214.28 MHz and has a bandwidth of 3.5%. He also proposed some other antennas among which there is a microstrip antenna for application in aircrafts. The antenna has a height of 0.16λ at the mean frequency and has a bandwidth of 25%.

King [27] derived expressions of the input impedance of an asymmetrically driven

antenna involving a series combination of the known impedances of symmetrically driven antennas. The sleeve monopole antenna was modelled as an asymmetrically driven dipole antenna applying the image theory. Then the input impedance of the sleeve antenna was computed at the elevated feed point. He then plotted the impedance frequency response of a sleeve dipole and compared that with the response of a conventional dipole. His results show that unlike the conventional dipole the sleeve dipole is a broadband antenna.

Burberry [28] discussed several sleeve antennas while presenting a review on aircraft antennas. Starting with the simple unipole he discussed the simple sleeve, the compensated sleeve and the bent sleeve antennas. The simple sleeve [Fig. 1.2(a)] is a straight vertical antenna where the outer conductor of the feeding coaxial cable is extended beyond the ground plane along some portion of the antenna. The compensated sleeve [Fig. 1.2(b)] is a simple sleeve antenna in which after the sleeve section, there is a small gap, and then the top radiator is covered with the outer conductor of the feed line. Using the compensated sleeve, a bandwidth of $2:1$ can be obtained. The bent sleeve antenna [Fig. 1.2(c)] is a slanted sleeve monopole with top half length bent. Such a bent sleeve monopole can be used in aircrafts within the frequency range of 200–400 MHz with a VSWR of $2:1$ or less.

Poggio *et al.* [29] investigated the radiation pattern of the sleeve monopole antenna experimentally. According to them the radiation pattern of a sleeve antenna primarily depends upon $l + L$ and $\frac{l}{L}$ where, length of top radiator portion is l and length of the sleeve portion is L. They designed a sleeve antenna which would operate within the frequency range of 100–400 MHz. To investigate the characteristics of the antenna they used the scale model measurement techniques [30]. In this

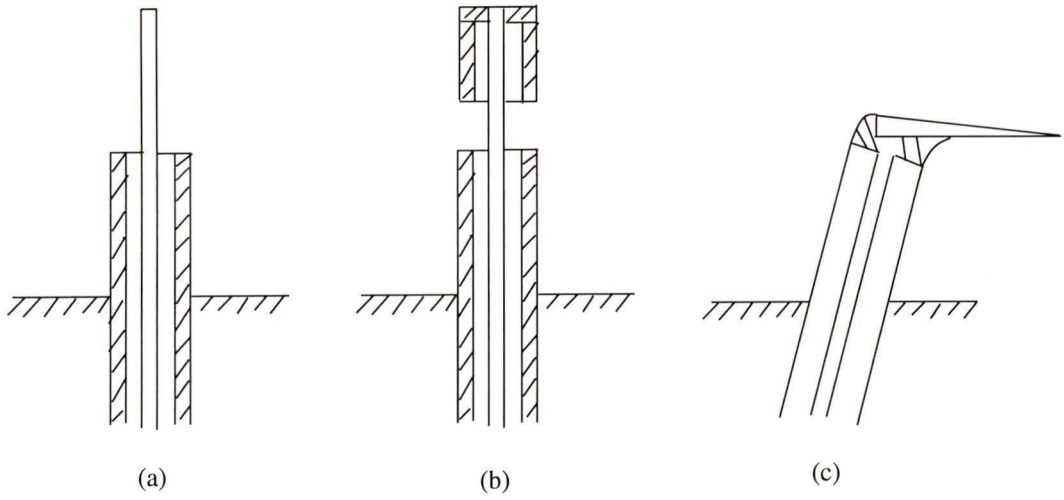

Figure 1.2: The sleeve antennas discussed by Burberry [28]. (a) The simple sleeve, (b) the compensated sleeve, and (c) the bent sleeve

technique the antenna designed for measurement is a scaled version of the original antenna. The scaled version can either be larger or smaller than the original antenna. If the scale model is smaller than the original antenna, then the following conditions are to be fulfilled [30] -

1. The linear dimensions of the model are $\frac{1}{n}$ times those of the full scale antenna.
2. The operating frequency and the conductivity of the materials used in the model are n times those of the full scale model
3. The complex permittivity and magnetic permeability of the materials used in the model are the same as in the full scale model

In the above, n is an arbitrary number which determines the scale factor of the model.

Poggio and his colleagues [29] experimented with a scale model that was smaller than the original antenna. Experiments were conducted within the frequency range of 500–2000 MHz. The antenna had a length of 0.208λ at the lowest frequency. They suggested that if $l + L \leq \frac{\lambda}{2}$, $\frac{l}{L}$ has almost no effect on the radiation pattern of the antenna. But as soon as $l + L$ exceeds $\frac{\lambda}{2}$, the pattern becomes markedly dependent upon $\frac{l}{L}$. The optimized $\frac{l}{L}$ for a uniform radiation pattern over a frequency range of $4 : 1$ was found to be 2.25. Within the entire frequency range, the VSWR was less than $8 : 1$.

Their experimental results show that the sleeve diameter has a negligible effect on the radiation pattern of the antenna which means that the sleeve antenna retains the original monopole radiation pattern almost entirely within a frequency range of $4 : 1$ even if the sleeve diameter is changed. It has been reported that with a $\frac{D}{d}$ (D is the sleeve diameter and d is the radiator diameter) of 7.0, the pattern shows some small sidelobes when the excitation frequency exceeds 1800 MHz. However, reduction in side lobe levels was obtained throughout the frequency range for a $\frac{D}{d}$ of 3.0.

King *et al.* [31] presented the experimental study of a balun-fed open-sleeve dipole in front of a metallic reflector. The antenna cross section is shown in Fig. 1.3 where D is the diameter of the antenna and the sleeves, S is the spacing between the antenna and the sleeve, L is the length of the sleeve, and H is the length of the antenna. This antenna was developed for a satellite antenna system and it operates within the frequency range of 225-400 MHz with a VSWR of $2.5 : 1$ or less.

This paper provides an excellent set of experimental design data which can be helpful in sleeve antenna design. Instead of making a hollow circular cylinder as a

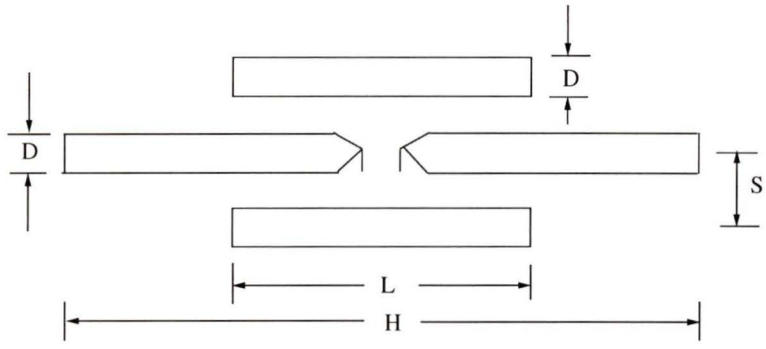

Figure 1.3: The open sleeve dipole of King *et al.* [31] (cross-section is shown)

sleeve, King and his colleague used two tubular conductors (the same as the dipole) as the sleeve. The sleeve length L and the spacing between the sleeve and the dipole S are the design variables. Their experimental results show that the design parameters can be varied to allow a wide range of choices between the VSWR performance and the bandwidth. The gain and the radiation pattern of the open-sleeve antenna are similar to those of a cylindrical sleeve antenna. They also have experimented with a cross dipole assembly to generate circular polarization.

Bailey [32] proposed a fan-dipole to be used in a planar array of half wavelength spaced elements operating over a ground plane. It operates within the frequency range of 500–700 MHz. It is a printed dipole on Teflon-fiberglass substrate and is fed by a balun. The best wide band impedance characteristics was achieved when the dipole length was about 0.3λ and the height of the balun was $\frac{3\lambda}{8}$. A bandwidth of 37% is reported to have been achieved for this antenna.

Nakano *et al.* [9] proposed zigzag and meander dipole configurations. A straight dipole antenna is bent to make those structures. They calculated the input impedance of a zigzag dipole using MoM. According to their results 34% shortening can be

achieved using the zigzag configuration in comparison to the straight dipole operating at the same frequency.

A shortening of 30% has been reported using the meander dipole configuration. The radiation pattern of the zigzag and the meander dipole was found to be similar to that of a conventional dipole. Both for the zigzag and the meander dipoles the gain and the half power beam width remains almost the same as that of the half-wave length dipole. Although the geometry of the zigzag and the meander suggests that there would be cross-polarization component present, their results show that within some design limits the cross-polarization is negligible [9].

Friedman[33] investigated a small disk loaded monopole antenna which is located 0.097λ above a ground plane with a top loaded disk of diameter 0.26λ . The impedance matching network consists of a biconical center post and two side posts located under the disk. The antenna operates within the frequency range of 300–650 MHz and has a bandwidth of $1.9 : 1$.

Wong *et al.* [10] proposed a meander monopole antenna with broadband characteristics. The antenna consists of a driven element fed from a coaxial line and one or more closely spaced open sleeves. Both the driven elements and the open sleeves are made from 2.06 mm diameter wire. The dual zigzag configuration was chosen to reduce cross polarization effect. Experiments were conducted in the frequency range of 250–750 MHz. The antenna was designed at a center frequency of approximately 400 MHz. At the center frequency the antenna has a height of 0.1862λ and has a width of 0.1542λ. The VSWR was less than $5.5 : 1$ within the measured frequency range.

They also measured the radiation pattern of the dual meander antenna on a 1.63λ diameter ground plane within the frequency range of measurement. The quarter wavelength monopole pattern is retained with the presence of small side lobes when the frequency exceeds 500 MHz.

Rashed *et al.* [11] proposed a new class of meander monopole antennas. This meander configuration is different than that proposed by Nakano et al. [9] because the antenna is meandered perpendicular to the meander axis for which current flows in the upward and in the downward directions in the vertical elements of the antenna. With the increase in the number of meander sections in the same period the shortening ratio decreases. But for a higher shortening ratio the radiation resistance as well as the bandwidth decreases. Also increased shortening ratio means increased wire length with ohmic losses in the wire which causes the reduction in radiation efficiency. They suggested that these antennas be used in Yagi-Uda antennas and in log-periodic dipole arrays.

Dey *et al.* [34] proposed a printed dipole antenna which operates within the frequency range of 1 to 2.1 GHz. It was fabricated on a dielectric substrate ($\epsilon_r = 4.2$, where ϵ_r is the dielectric constant of the substrate) to operate at a center frequency of 1.5 GHz. The antenna has a length of $0.475\lambda_d$ ($\lambda_d = \frac{\lambda}{\sqrt{\epsilon_r}}$) and the feed line length is $0.553\lambda_d$. They have used a matching stub to increase the bandwidth of the antenna. By varying the stub position a bandwidth of 48% has been reported.

Rashed [12] also proposed a meander line section as a monopole antenna. This antenna looks like a folded unipole which has periodic expansion along the axis of the ground plane. In this configuration if the lateral expansion is comparable to the vertical element then there would be horizontally polarized field components present.

He investigated numerically and experimentally the impedance, the bandwidth and the radiation pattern of the antenna. For this configuration, the radiation resistance and the bandwidth decreases with increasing shortening ratio.

Nakano *et al.* [35] [36] used the method of moments to calculate the impedance and the radiation characteristics of printed zigzag and meander dipole antennas. Those antennas were etched on dielectric substrates and the ground planes beneath the substrates were not etched off. The substrate thickness is $0.1016\lambda_0$ and the printed wire has a radius of $10^{-4}\lambda_0$, where λ_0 is the wavelength corresponding to the resonant frequency. The resonant frequency is defined as the frequency when the input reactance of an antenna is zero [8]. A shortening of 47% was achieved with the meander dipole on a substrate with dielectric constant of 2.0. The same antenna has a shortening ratio of 68% on a substrate with dielectric constant of 6.05.

Yu *et al.* [4] investigated printed circuit dipole antennas for the application in personal communication network (PCN) handset. Duroid 6010 substrate with a dielectric constant of 10.5 and a thickness of 0.064 cm was used for the printed antenna configurations and the ground conductor was etched off. For a printed meader dipole with a length of 11.2 cm the bandwidth is 7.3% at a center frequency of 880 MHz. The corresponding shortening ratio of this antenna is 34.1%.

To achieve further shortening they have used another layer of the same substrate with the same thickness. The meander antenna was sandwiched between the two layers of dielectric substrate. Such a sandwiched meander dipole has a length of 9.2 cm, with a shortening ratio and bandwidth of 45.9% and 5.0% respectively.

1.4 Outline of The Thesis

This thesis has been organized as follows -

In Chapter 2 the theory of the straight monopole antennas is presented. Topics like radiated fields, input impedance, bandwidth, efficiency, polarization etc. are discussed for the straight thin monopole. Since the input impedance is the only parameter that varies widely with the increase in wire diameter [7], the methods to calculate it for a thick antenna are mentioned and simplified expressions for the same are presented.

Since our interest was in bent linear antennas, several such antenna configurations are then discussed. The configurations considered under this heading are - the zigzag and the meander. The term *'shortening ratio'* and the design parameters for those antennas are defined. As a prior step to designing a broadband sleeve antenna, the principles of the sleeve antenna and some of its characteristics are discussed. The design variables for the sleeve antenna are also defined and the design constraints discussed.

In Chapter 3 the input impedance and the VSWR of a straight thin and a thick antenna are calculated. The impedance and the VSWR frequency responses of these two antennas are then compared to demonstrate the effect of radius on those. The assumptions and the design considerations for the meander and the dual meander antenna are presented. A new type of antenna, the *sinusoidal antenna*, is proposed and the design limits of this antenna are discussed exploiting its similarity with the zigzag antenna. The advantages of using a printed bent antenna are pointed out and its design constraints discussed.

A broadband sleeve antenna is designed at a single frequency using the concept of an equivalent circuit. Referring to King *et al.* [31] it has been proposed that instead of using a hollow circular cylindrical sleeve, two posts be used as sleeves and their appropriate lengths be selected by observing the VSWR.

In Chapter 4 experimental objectives and procedures are discussed. Experimental arrangements are shown in block diagrams and measurement equipment and measuring principles are described in detail.

In Chapter 5 the experimental results of bent wire antennas, printed bent antennas, and the sleeve antennas are presented. The results for the bent wire antennas are presented in two different subsections: Thick Bent Antennas and Thin Bent Antennas. In the first subsection the measured input impedances and the VSWR's of a meander, a sinusoidal, and a straight antenna are presented. The shortening effect and the narrowing of the bandwidth in bent antennas are demonstrated. In the second subsection the results found from the investigation of a number of wire sinusoidal and wire meander antennas are presented. The VSWR frequency characteristics and the shortening ratios of the meander and the sinusoidal configuration are then compared.

Under the section heading 'Printed Bent Antennas' the shortening ratio and the bandwidth characteristics of a printed meander and a sinusoidal antenna are discussed. Finally, the bandwidth characteristics of a straight sleeve and a dual meander sleeve antenna are discussed.

In Chapter 6 experimental results are discussed and compared. A new explanation of the phenomenon of shortening in bent antennas is proposed. Then the

advantages and limitations of the newly developed antennas are pointed out. Suggestions for improvements of characteristics are also given along with the possible future course of work in this area. Finally, the thesis is closed by the concluding remarks.

Chapter 2

Theory

In this thesis several bent antenna configurations, e.g. the meander, the sinusoidal, and the dual meander have been experimentally investigated by operating those as vertical monopoles. Therefore, it is expected that the radiation characteristics, like, radiation pattern, input impedance, bandwidth, polarization, efficiency etc. of these antennas would be similar to those of a straight vertical monopole [9], [11], [10]. Hence, before we proceed with the theory and the design constraints of bent antennas, a brief theory of the straight wire monopole would be relevant and useful.

2.1 Straight Monopole Antennas

The electrical properties of monopole antennas are dependent both upon the geometry of the antenna element and the ground plane. Let us consider a straight

vertical monopole on a ground plane of infinite extension. It is well known that such an antenna can be modelled as a center-fed dipole by applying the image theory. It would radiate over the upper hemisphere of the ground plane with half the input impedance and twice the peak directivity of a center-fed dipole [25].

2.1.1 The Thin Monopole Antenna

A linear antenna can be defined as a thin or a thick antenna depending upon its length to radius ratio. Weiner *et al.* [25] defines an antenna as a thin antenna if its length to radius ratio is much greater than 10^4 or a relatively thick antenna if its length to radius ratio is from 10^1 to 10^4. Let us consider a thin antenna at the center of a perfectly conducting, infinitely thin, infinite ground plane [Fig. 2.1(a)]. The antenna is radiating in free space.

The electrical characteristics of such an antenna are a function of only two parameters, namely, the element length and the element radius normalized to the excitation wavelength. The antenna is fed by a coaxial line with its inner conductor connected to the vertical monopole element through a hole in the ground plane and its outer conductor connected to the ground plane by a flange. The antenna of Fig. 2.1(a) is modelled as a dipole by image theory in Fig. 2.1(b). For the dipole in Fig. 2.1(b), the current distribution can be assumed to be sinusoidal and can be expressed as [7]

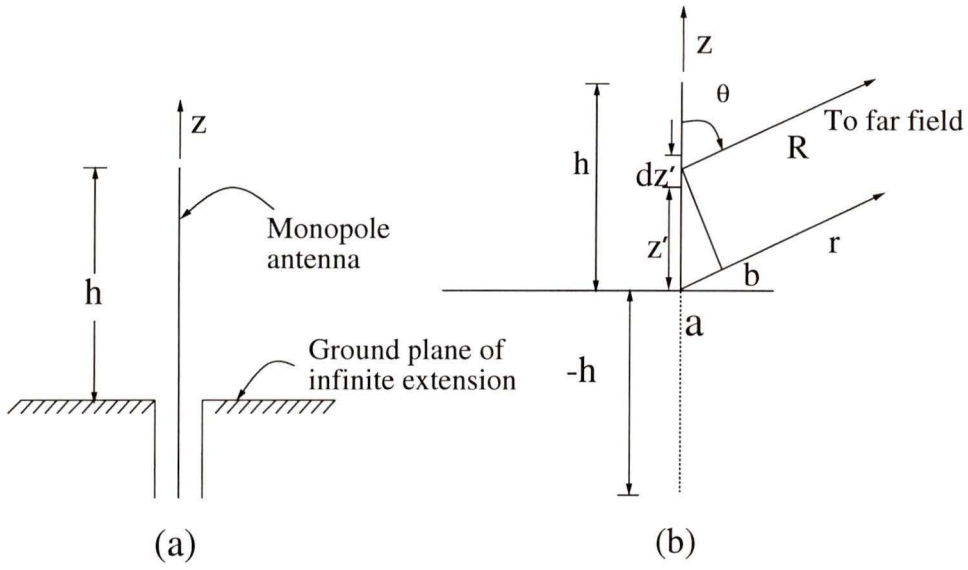

Figure 2.1: (a) A straight thin monopole antenna on infinite ground plane, (b) the same antenna when modelled as a dipole by applying image theory

$$I(z') = \begin{cases} \hat{a_z} I_o \sin[k(h-z)] & \text{if } 0 \leq z \leq h \\ \hat{a_z} I_o \sin[k(h+z)] & \text{if } -h \leq z \leq 0 \end{cases} \tag{2.1}$$

where I_o is the maximum amplitude of the current, k is the free space wave number and h is the height of the antenna above the ground plane.

Fields and Radiation Pattern

Let us assume that the current vanishes at the end points of the antenna ($z = \pm h$). Let us then subdivide the dipole of Fig. 2.1(b) into a number of infinitesimal dipoles of length $\Delta z'$ [7]. With a higher number of subdivisions, the infinitesimal dipole approaches a length dz'. Now, for that infinitesimal element positioned along the z

axis at z', the electric and the magnetic field components in the far field are given by

$$dE_\theta \simeq j\eta \frac{kI(z')}{4\pi R} e^{-jkR} \sin\theta dz' \tag{2.2}$$

$$dE_r \simeq dE_\phi = dH_r = dH_\theta = 0 \tag{2.3}$$

$$dH_\phi \simeq j \frac{kI(z')}{4\pi R} e^{-jkR} \sin\theta dz' \tag{2.4}$$

In the far-field, the following assumptions are valid [7]

- for phase terms, $R \simeq r - z' \cos\theta$
- for amplitude terms, $R \simeq r$

where $r = \sqrt{x^2 + y^2 + z^2}$, x, y, z are the observation point coordinates and x', y', z' are the source point coordinates, and η is the intrinsic impedance of the medium; in free space $\eta = 377\ \Omega$. Now,

$$dE_\theta \simeq j\eta \frac{kI(z')}{4\pi r} e^{-jkr} \sin\theta e^{jkz' \cos\theta} dz'. \tag{2.5}$$

Summing the contributions of all the infinitesimal elements, within the limits the summation leads to an integration

$$E_\theta = j\eta \frac{k}{4\pi r} e^{-jkr} \sin\theta [\int_{-h}^{h} I(z') e^{jkz' \cos\theta} dz']. \tag{2.6}$$

The factor outside the bracket in (2.6) is called the element factor and that inside the bracket is called the space factor. The element factor depends upon the type of current and its direction of flow while the space factor is a function of the current distribution along the source. After some mathematical manipulations (2.6) can be expressed as [7]

$$E_\theta \simeq j\eta \frac{I_o}{2\pi r} e^{-jkr} [\frac{\cos(kh\cos\theta) - \cos(kh)}{\sin\theta}],\ 0 \leq \theta \leq \frac{\pi}{2} \tag{2.7}$$

And the expression for the magnetic field is

$$H_\phi \simeq \frac{E_\theta}{\eta} \tag{2.8}$$

The electric and or the magnetic fields can then be calculated and plotted using (2.7) and (2.8).

The performance of an antenna is often expressed in terms of $\vec{E}$ or and $\vec{H}$ plane patterns [7]. For a linearly polarized antenna the $\vec{E}$ plane pattern is defined as the plane containing the electric field vector and the direction of maximum radiation. It is also called the elevation plane pattern. The elevation plane pattern is plotted in the elevation plane with a specific ϕ value. Similarly, for a linearly polarized antenna the $\vec{H}$ plane pattern is defined as the plane containing the magnetic field vector and the direction of maximum radiation. It is also called the azimuthal plane pattern. The azimuthal plane pattern is plotted in the azimuth plane with a specific θ value.

Input Impedance and Bandwidth

The input impedance of an antenna is defined as the impedance presented by it at its input terminals which can be expressed as the ratio of the voltage to current at that terminal [7]. The input impedance of an antenna can be expressed as

$$Z_{in} = R_{in} + jX_{in} \tag{2.9}$$

where, R_{in} is the input resistance and X_{in} is the input reactance. Balanis [7] derived the expression of the input impedance of a center-fed dipole. The input resistance

of a thin linear antenna assuming it to be lossless ($R_L = 0$) can be expressed as [7]

$$R_{in} = \frac{R_r}{\sin^2(kh)} \tag{2.10}$$

where, R_r is the radiation resistance by which the antenna radiates its power. Therefore, to derive an expression for R_{in}, we need an expression for R_r. Now, to derive the expression for R_r, the following steps are to be followed [7]

1. The expression for the time average Poynting vector, $\vec{W_{av}} = \frac{1}{2}\Re[\vec{E} \times \vec{H}]$ is to be derived using equation (2.7) and (2.8).

2. $\vec{W_{av}}$ is then to be integrated over the volume of a sphere of radius r to have an expression for the radiated power, P_{rad}.

3. As soon as the expression for the total radiated power is derived, R_r can be calculated using the equation $R_r = \frac{2P_{rad}}{|I_o|^2}$

The derivation of the expression of the input reactance involves the expression of the near zone fields of the antenna which can be derived by the 'Induced EMF Method' [7]. Weiner *et al.* [25] have formulated the expressions for the input resistance and the input reactance of a thin monopole antenna on infinite ground plane using similar expressions from [7] derived for thin dipole antennas.

$$\begin{aligned} R_{in} \;=\; & \frac{\eta}{4\pi \sin^2 kh}\{\mathrm{Cin}\,(2kh) + \\ & \frac{1}{2}\sin(2kh)[\mathrm{Si}\,(4kh) - 2\mathrm{Si}\,(2kh)] + \\ & \frac{1}{2}\cos(2kh)[2\mathrm{Cin}\,(2kh) - \mathrm{Cin}\,(4kh)]\} \end{aligned} \tag{2.11}$$

$$
\begin{aligned}
X_{in} \;=\; & \frac{\eta}{4\pi \sin^2 kh}\{\mathrm{Si}\,(2kh) + \\
& \cos(2kh)[\mathrm{Si}\,(2kh) - \frac{1}{2}\mathrm{Si}\,(4kh)] - \\
& \sin(2kh)[\ln(h/b) - \mathrm{Cin}\,(2kh) + \\
& \frac{1}{2}\mathrm{Cin}\,(4kh) + \frac{1}{2}\mathrm{Cin}\,(kb^2/h)]\}
\end{aligned} \tag{2.12}
$$

where, b is the wire radius in wavelength, $\mathrm{Cin}\,(x)$ is the modified cosine integral, and $\mathrm{Si}\,(x)$ is the sine integral

$$\mathrm{Cin}\,(x) = \int_0^x (1 - \cos p)\frac{dp}{p} \tag{2.13}$$

$$\mathrm{Si}\,(x) = \int_0^x \frac{\sin p}{p} dp \tag{2.14}$$

Now, if the input impedances of the antenna within a desired frequency range are known, and if we assume that the antenna is fed by a 50Ω coaxial cable, then

$$\Gamma = \frac{Z_{in} - 50}{Z_{in} + 50} \tag{2.15}$$

$$VSWR = \frac{1 + |\Gamma|}{1 - |\Gamma|} \tag{2.16}$$

where Γ is the complex reflection coefficient and $|\Gamma|$ is its magnitude.

Efficiency

The overall efficiency of an antenna can be expressed as [7]

$$\%e_t = e_r e_{cd} \times 100 = (1 - |\Gamma|^2)\,\frac{R_r}{R_r + R_L} \times 100 \tag{2.17}$$

where, $e_r = (1 - |\Gamma|^2)$ is the reflection efficiency and $e_{cd} = \frac{R_r}{R_r + R_L}$ is the conduction dielectric efficiency. For a linear antenna, R_L is expressed as [7]

$$\frac{l}{2\pi b}\sqrt{\frac{\omega\mu}{2\sigma}} \tag{2.18}$$

where, $\mu = 4\pi \times 10^{-7}$ H/m in free space, $\sigma = 5.7 \times 10^7$ S/m for copper, l is the wire length, b is the wire radius.

Polarization

Polarization of an antenna in a given direction is defined as the polarization of the radiated wave when the antenna is excited [7]. Polarization of a radiated wave is defined as the figure traced by the extremity of the electric field vector as a function of time at fixed location in space and the sense in which it is traced. Polarization can be linear, circular or elliptical. If the time varying vector that represents the electric field at a point in space is always directed along a line, the field is said to be linearly polarized.

Let us consider the field of a plane wave travelling in the negative z-direction,

$$\vec{E}(z,t) = \hat{a_x}E_x(z,t) + \hat{a_y}E_y(z,t) \tag{2.19}$$

where

$$E_x(z,t) = E_x\cos(\omega t + kz + \phi_x) \tag{2.20}$$

$$E_y(z,t) = E_y\cos(\omega t + kz + \phi_y) \tag{2.21}$$

where, E_x and E_y are the maximum magnitudes of the x and y components of the $\vec{E}$ fields, ϕ_x, and ϕ_y are the associated phases and ω is the angular frequency. Polarization can be of three types-

Linear Polarization: $\Delta\phi = \phi_y - \phi_x = n\pi$, $n = 0, 1, 2, 3, \ldots$

Circular Polarization: $E_x = E_y$ and $\Delta\phi = \phi_y - \phi_x = \pm(4n+1)\frac{\pi}{2}$, $n = 0, 1, 2, 3, \ldots$

Elliptic Polarization: $E_x \neq E_y$ when $\Delta\phi = \phi_y - \phi_x = \pm(4n+1)\frac{\pi}{2}$ or $\Delta\phi = \pm\frac{n\pi}{2} >$ 0 *or* < 0, $n = 0, 1, 2, 3, \ldots$

A straight monopole antenna radiates linearly polarized waves. Linear polarization can be horizontal or vertical or arbitrary. A straight vertical monopole antenna radiates vertically polarized waves. Similarly, a straight horizontal monopole antenna radiates horizontally polarized waves.

2.1.2 The Thick Monopole

A very thin linear antenna is narrowband. The narrowband characteristic of a thin linear antenna can be understood from its impedance frequency response. For such an antenna any small perturbations in the operating frequency results in a large change in its input impedance making the wideband matching of the impedance difficult.

By increasing the diameter of the wire or by decreasing the l/d ratio the input impedance of such an antenna can be made less sensitive to frequency change. As a result the impedance of a thick antenna can be matched over a wide range of frequencies. For example, an antenna with a $l/d = 5000$ has a bandwidth of about 3%, whereas an antenna with the same length but with a $l/d = 260$ has a bandwidth of approximately 30% [7].

The input impedance of a thick antenna can be calculated by several methods [14] – (a) The method of moments, (b) the induced EMF method, (c) Storer's variational solution, (c) zeroth and first order solution to Hallen's equation, (d) King Middleton second order solution etc.

The application of the method of moments to determine the input impedance only is not a good choice [14]. Application of the method of moments involves large matrices which are solved for the unknown current distribution. To compute only the input impedance of an antenna, the input current instead of the complete current distribution is needed. Therefore, in such a case, other simplified methods can be used. Applying the induced EMF method the input impedance of a cylindrical dipole can be expressed as [14]

$$Z = \frac{j60}{\sin^2(kl)}\{4\cos^2(kl)\,\mathrm{S}\,(kl) - \cos(2kl)\mathrm{S}\,(2kl) - \sin(2kl)[2\mathrm{C}\,(kl) - \mathrm{C}\,(2kl)]\} \quad (2.22)$$

where

$$\mathrm{C}\,(kl) = \ln(\frac{2l}{a}) - \frac{1}{2}\mathrm{Cin}\,(2kl) - \frac{j}{2}\mathrm{Si}\,(2kl) \quad (2.23)$$

and

$$\mathrm{S}\,(kl) = \frac{1}{2}\mathrm{Si}\,(2kl) - \frac{j}{2}\mathrm{Cin}\,(2kl) - ka, \quad (2.24)$$

$\mathrm{Si}\,(x)$ and $\mathrm{Cin}\,(x)$ are the sine and modified cosine integrals defined by equations (2.13) and (2.14) respectively. C. T. Tai [14] has found that the computed Z from equation(2.22) fits very well in the range $0 \leq 2l/\lambda \leq \pi/2$ by the expression –

$$Z = R(kl) - j[120(\ln\frac{2l}{a} - 1)\cot kl - X(kl)] \quad (2.25)$$

where, the R(kl) and X(kl) are functions tabulated and graphed in [38].

A further modification of Tai's expression for the range of $1.3 \leq kl \leq 1.7$ and $.001588 \leq \frac{a}{\lambda} \leq .009525$ has been done [14] by representing R(kl) and X(kl) by second

degree polynomials with coefficients chosen to fit data computed from (2.22). The resulting expression for the input impedance of a thick antenna is

$$Z = [122.65 - 204.1kl + 110(kl)^2] - j[120(\ln(\frac{2l}{a} - 1)\cot kl - 162.5 + 140kl - 40(kl)^2] \tag{2.26}$$

where l is the half length of the dipole antenna and a is the radius of the wire. The simplified expression does not introduce much error in comparison to the more exact formulation of (2.22). The input impedance of a coaxial fed monopole antenna when radiating over an infinite ground plane would simply be half of Z in equation (2.22) or (2.26).

2.2 Bent Linear Antennas

Linear antennas need not be straight dipoles or monopoles. They can be bent. One reason for deforming a straight monopole or dipole is to shorten its length. So far three types of bent linear antennas, the zigzag antenna, the meander antenna, and the dual meander antenna have been investigated [9], [11], [12] [10]. Several such antennas are shown in Fig. 2.2, 2.3, and 2.4. According to any of these figures L_{ax} is the length of any bent monopole antenna.

Now let us consider a straight monopole of length L that operates at the same center frequency as the bent monopole. Since it is well known that $L_{ax} < L$, [9] a parameter of merit known as the *shortening ratio* can be defined as

$$\% \, SR = \frac{L - L_{ax}}{L} \times 100 \tag{2.27}$$

where SR is the abbreviation of the shortening ratio.

2.2.1 The Zigzag Antenna

Two bent antennas are shown in Fig. 2.2. They follow the same geometric pattern with different axial length, periodicity, and amplitude. These antennas correspond to the zigzag antennas investigated by Nakano and his associates [9] except that these are monopole antennas. They can be made by bending a wire or by etching the configuration over a dielectric substrate.

According to Fig. 2.2 the zigzag antenna resembles a triangular waveform. It has an amplitude A, a period P, and an axial length L_{ax}. The total wire length L_{wire}, the edge angle τ and the segment lengths can be calculated by using the design variables A, P, and L_{ax}. For example - if we want an antenna to have an axial length of 5 cm, a period of 1 cm, and an amplitude of 1 cm, the total wire length, each segment length and edge angle would be 21.25 cm, 1.06 cm, and 28° respectively.

2.2.2 The Meander Antenna

The meander antenna shown in Fig. 2.3 is due to Nakano *et al.* [9] except that it is a monopole. All the segments of the meander antenna in Fig. 2.3 have equal lengths e. A considerable amount of shortening can be achieved by using this geometry with a comparable radiation resistance to that of a straight wire monopole. For example a shortening of 30% can be achieved with $e = 0.0133\lambda$ and radiation resistance of 21.5 Ω. Like the zigzag antenna this antenna can be made either by bending a wire or by printing a strip on a dielectric substrate.

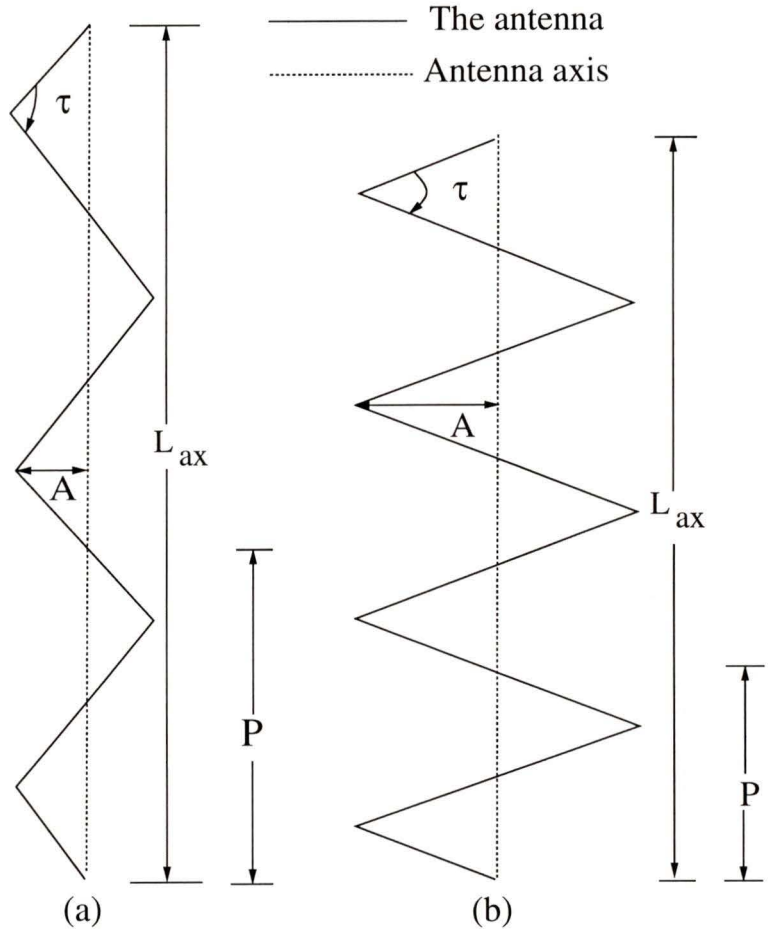

Figure 2.2: The geometry of the zigzag antenna

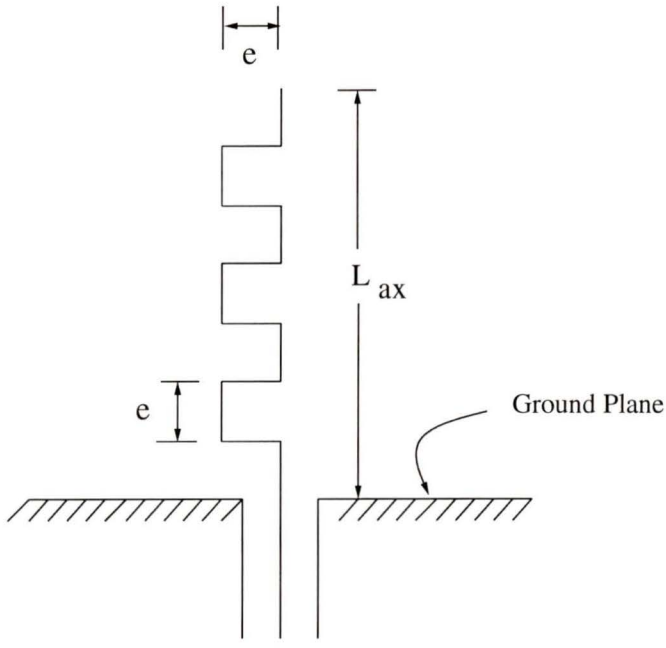

Figure 2.3: A meander antenna configuration

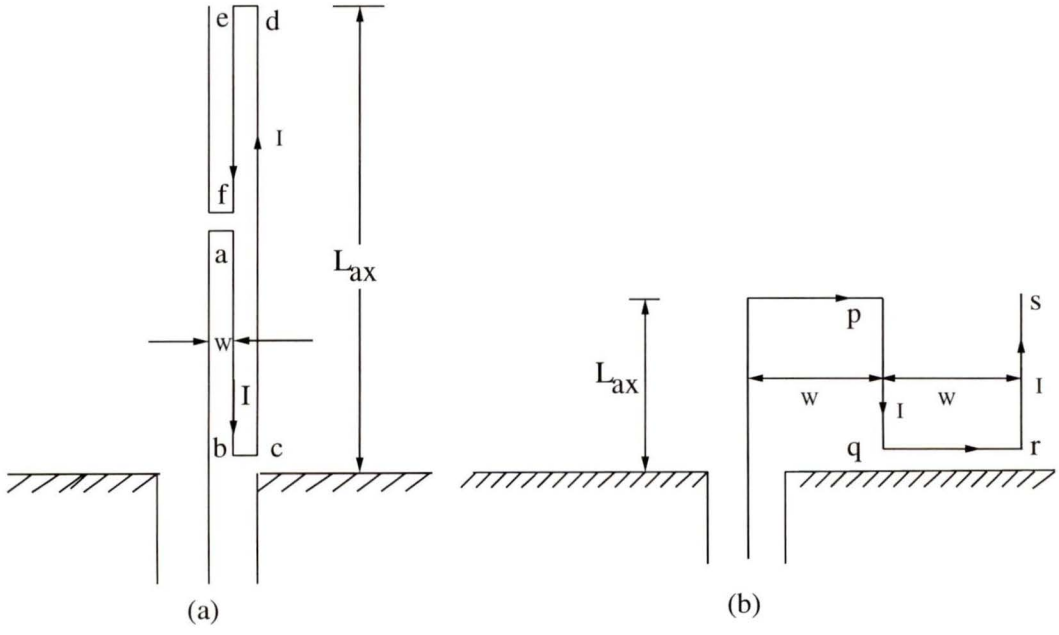

Figure 2.4: Other meander antenna configurations

The meander antennas in Fig. 2.4(a) and 2.4(b) are due to Rashed *et al.* [11] and Rashed [12]. The length of both the antennas is L_{ax} and the separation between two vertical elements is w. For the antenna in Fig. 2.4(a), the shortening ratio depends upon the number of meander sections per wave length N, (in Fig. 2.4(a) $N = 4$) and width w. Increased shortening (of the order of 41% or more) can be achieved by using fewer number of meander sections ($N = 2$) but at the expense of very low radiation resistance and bandwidth [1] (of the order of 13 Ω and 3%).

The antenna in Fig. 2.4(b) has a small separation $w \ll l$. Increased shortening can be achieved by increasing w until the cross-polarization constraint is exceeded. But increased shortening means very low radiation resistance and bandwidth. For example - an antenna with $w = 0.25$ cm, wire length of 13.5 cm, wire radius of 0.4 mm has a radiation resistance of 14.2 Ω, a shortening ratio of 36% and a bandwidth of 3.6% at a resonant frequency of 976 MHz.

In Fig. 2.4(a) the current in segment ab and ef are in opposite directions to the current in segment cd. Similarly, in Fig. 2.4(b) the current in segment pq is in opposite direction to that in segment rs. The currents in all these segments are shown using arrows. Although each of the vertical sections would produce appreciable radiated fields, according to (2.6) there would be radiation cancellation in the far field due to these oppositely directed currents in the meandered wire because $w \ll \lambda$.

[1] Bandwidth for [11] and [12] is defined as "The input impedance curves are normalized to their resonant resistance values. A VSWR=2 circle is then used to find the upper and lower frequencies"

2.3 The Sleeve Antenna

The sleeve antenna is essentially an antenna in which the outer conductor of the feeding coaxial cable is stretched beyond the ground plane. Several such antennas are shown in Fig. 2.5. The sleeve is a broadband antenna. The bandwidth of a sleeve antenna can be as wide as 4 : 1 [29]. The VSWR over the entire frequency range is comparatively low because the sleeve provides smooth impedance frequency response [27].

Another important advantage of the sleeve antenna is, if properly designed, it can retain the original monopole pattern over a frequency range of 4 : 1 [29]. It may be mentioned that a straight quarter wavelength monopole is not capable of preserving the basic pattern when the bandwidth exceeds an octave [10].

The theoretical investigation of the sleeve antennas dates back to King [27]. He analyzed the sleeve antenna as an asymmetrically driven dipole and computed the currents and impedances over a range of frequencies. Because of the complicated structure of the sleeve antenna [Fig. 2.5(c)], most researchers [29], [31] employed experimental rather than analytical or numerical methods to investigate its characteristics.

According to Fig. 2.5 the sleeve length is a variable. It can vary from zero to the whole length of the antenna. The exterior part of the sleeve acts as a radiating element and the inside acts as the outer conductor of the feeding coaxial cable [8]. For the sleeve antenna configuration of Fig. 2.5(c) L is the sleeve length, D is the sleeve diameter, d is the radiator diameter, and l is the radiator length beyond the sleeve.

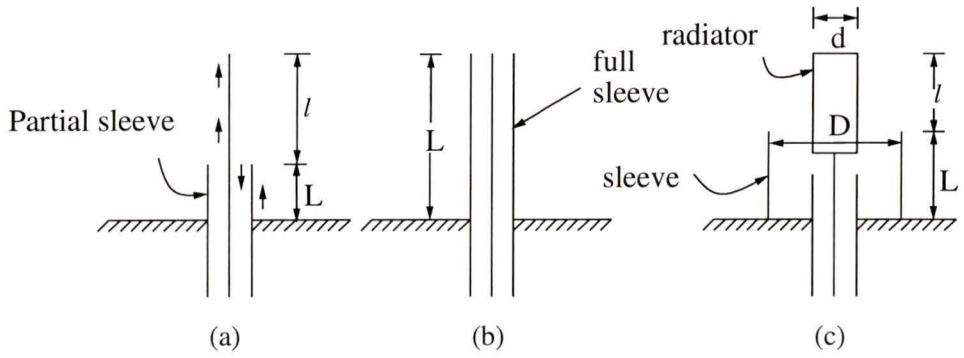

Figure 2.5: (a) A typical sleeve antenna, (b) a full sleeve antenna, and (c) the most common sleeve antenna

The design of a hollow circular cylindrical sleeve proceeds by locating the lower end of the frequency band near the first resonance. Thus the total length of the antenna, $l + L$ is fixed [8]. The remaining design variables are $\frac{l}{L}$, D or $\frac{D}{d}$. As long as $l + L \leq \frac{\lambda}{2}$, the radiation pattern of the antenna remains unaffected [8].

But if it is needed that the antenna has to operate within a frequency range of $4 : 1$ or $3 : 1$, the radiation pattern will be affected unless the best $\frac{l}{L}$ and $\frac{D}{d}$ are chosen which can be done experimentally. In the longer electrical lengths $\frac{l}{L}$ becomes very important because the current on the sleeve exterior may not be in phase with the current on the radiator. Experimental optimization of $\frac{l}{L}$ is necessary to decrease side lobe levels resulting from out of phase currents on the sleeve exterior.

An approximate equivalent circuit of the sleeve antenna of Fig. 2.5(a) is shown in Fig. 2.6 [39]. The antenna has three impedance components R, X_C and Z_o, where R indicates the impedance at the virtual feed point and is expressed as

$$R = \frac{R_o}{\cos^2 \theta} \tag{2.28}$$

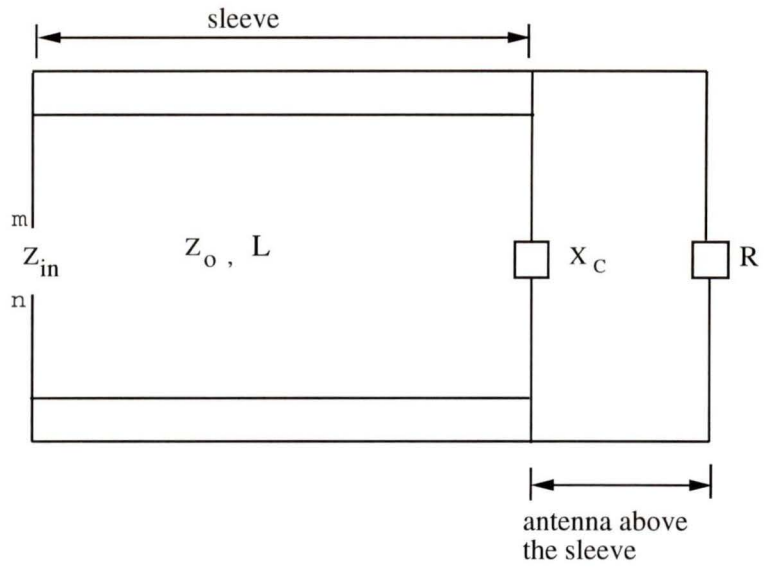

Figure 2.6: The approximate equivalent circuit of a sleeve monopole antenna

$$\theta = \beta L = \frac{2\pi L}{\lambda} \tag{2.29}$$

where R_o is the base impedance of the antenna element alone at resonance, X_c stands for the capacitive reactance that comes into existence due to the discontinuity between the sleeve end and the radiator, L indicates the transmission line length formed by the sleeve and the radiator [Fig. 2.5(a)] and Z_o is the characteristic impedance of that line.

Chapter 3

Calculations and Design

3.1 Radiation Characteristics of Straight Wire Antennas

3.1.1 The Thin Monopole Antenna

The input impedance of a thin (length to radius ratio greater than 10^4) monopole antenna can be calculated using equations (2.11) and (2.12). If a thin monopole with a wire diameter of 16.7×10^{-6} cm is designed to operate at a center frequency of 880 MHz, its length would approximately be 8.4 cm [8]. To calculate the input impedance, the sine and the modified cosine integrals of equation (2.13) and (2.14) were approximated as [40]

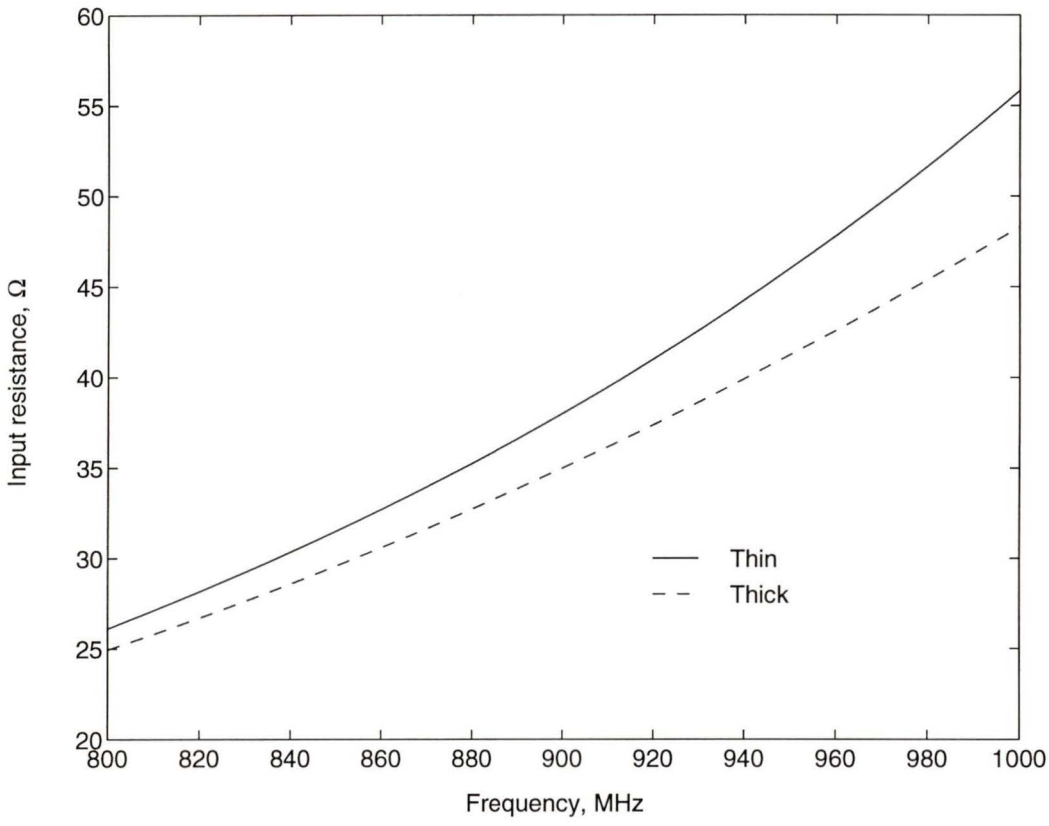

Figure 3.1: Input resistance vs frequency characteristics of straight monopole antennas

$$\mathrm{Si}\,(x) = x - \frac{x^3}{3!3} + \frac{x^5}{5!5} - \frac{x^7}{7!7} + \frac{x^9}{9!9} - \cdots + \frac{x^{33}}{33!33} \tag{3.1}$$

and

$$\mathrm{Cin}\,(x) = \frac{x^2}{2!2} - \frac{x^4}{4!4} + \frac{x^6}{6!6} - \frac{x^8}{8!8} + \cdots - \frac{x^{32}}{32!32} \tag{3.2}$$

The input resistance and reactance calculated within the frequency range of $800 - 1000$ MHz are plotted against frequency in Fig. 3.1 and 3.2.

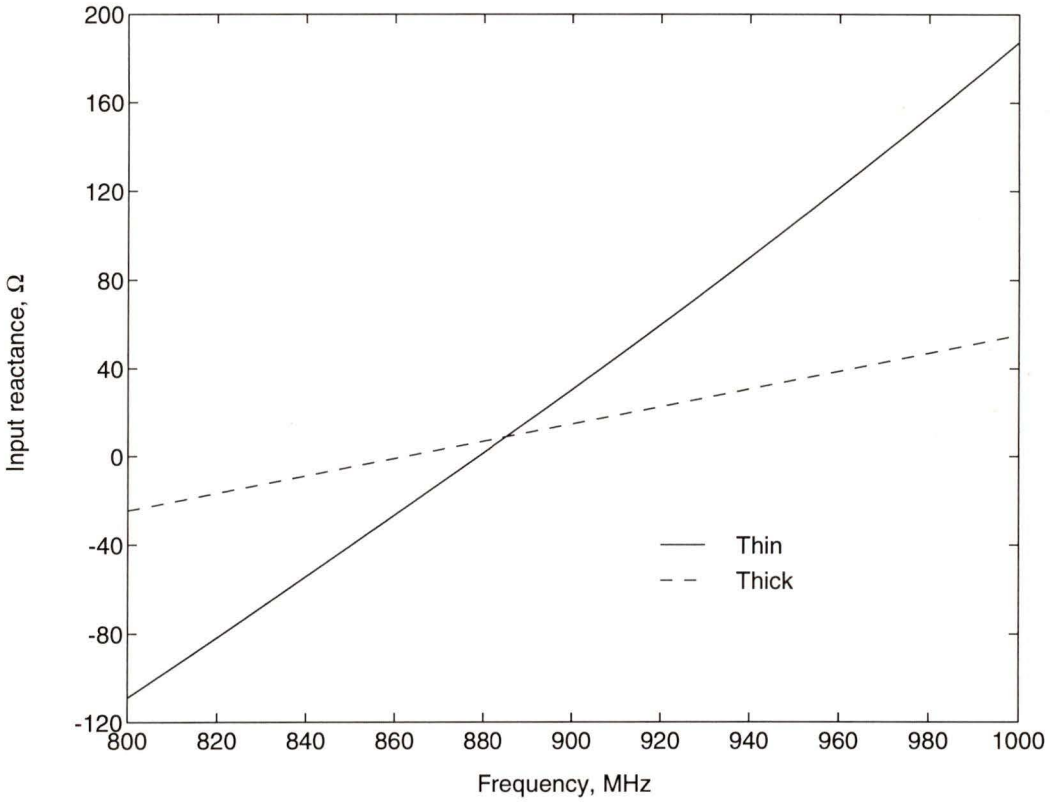

Figure 3.2: Input reactance vs frequency characteristics of monopole antennas

3.1.2 The Thick Monopole Antenna

Let us consider that a straight thick (length to radius ratio between 10^1 to 10^4) monopole antenna with a wire diameter of 2.5 mm is to be operated at around 880 MHz. Its approximate length should be 8.2 cm [8]. Input impedance of such an antenna within the frequency range of $800 - 1000$ MHz can be calculated using (2.26). The input resistance and reactance calculated are plotted against frequency in Fig. 3.1 and 3.2.

3.1.3 Comparison Between Two Straight Antennas

If the frequency response of the thin and the thick [see Fig. 3.1 and 3.2] antenna are compared, it can easily be seen that the variation of input impedance with frequency is much less for the thick antenna than that for the thin antenna. The input reactance for the thin antenna varies between $-110\,\Omega$ to $190\,\Omega$ whereas that for the thick antenna varies between $-25\,\Omega$ to $55\,\Omega$ within the same frequency range. The input resistance changes from $26\,\Omega$ to $56\,\Omega$ for the thin antenna whereas that for the thick antenna changes from $24\,\Omega$ to $47\,\Omega$. Using the input impedance for both the thin and the thick antenna, the VSWR was calculated applying (2.15) and (2.16). The VSWR frequency responses of these two antennas are then compared in Fig. 3.3. According to Fig. 3.3 the bandwidth of the thick antenna is 13% whereas that of the the thin antenna is 4%.

3.2 Design Considerations of Bent Antennas

Depending upon the shortening ratio and the radiation characteristics (bandwidth, polarization, radiation pattern etc.) required , a wide variety of bent antennas can be designed by varying the design variables, e.g. A and P [Fig. 2.2] or e and w [Fig. 3.4(a)]. But by changing these design parameters some of the important characteristics of these bent antennas also change. Therefore, it is important to learn about the design constraints of bent antennas before they are investigated.

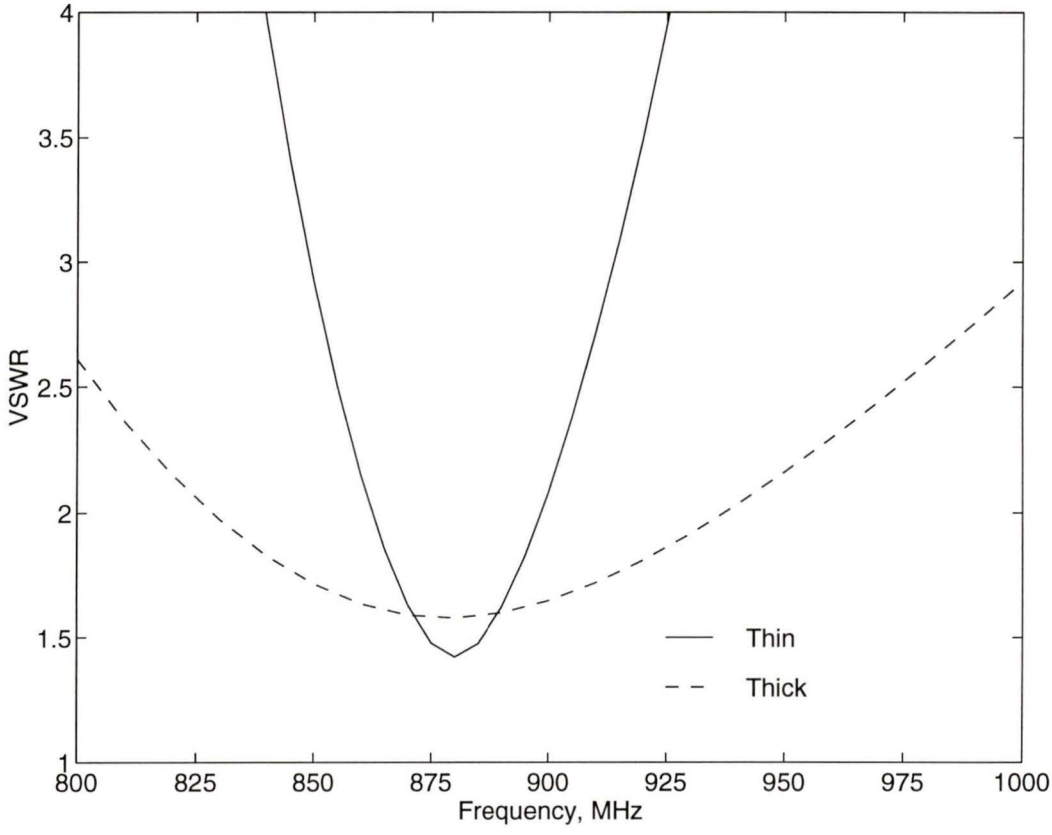

Figure 3.3: Comparison between the VSWR frequency characteristics of a thin and a thick monopole

Table 3.1: Experimental results of Rashed *et al.* [11] corresponding to the configuration in Fig. 2.4(a); L_{ax} = 4.5 cm, L_{wire} = 13.5 cm, w = 0.3 cm, wire radius, a = 0.4 mm

Antenna Type	*N*	*% Band Width*	*% SR*	R_{res}, Ω	f_o, MHz
Monopole	–	9.5	0	36.0	545
Meander1	2	3.0	41	13.0	922
Meander2	6	7.0	33	20.5	1050
Meander3	10	7.5	29	22.0	1110
Meander4	14	8.0*	25	23.5	1180

3.2.1 Bent Wire Antennas

The Wire Meander Antenna

We limited our investigation of meander antennas for a PCN handset within the geometry of Fig. 2.3 instead of the configurations in Fig. 2.4(a) and 2.4(b) for the following reasons –

- As mentioned earlier in section 2.2.2, due to the current flow in opposite directions in the vertical elements of the meandered wire, there would be considerable radiation cancellation in the far field for the configuartion in Fig. 2.4(a) and 2.4(b) because $w \ll \lambda$.

Table 3.2: Numerical results of Nakano *et al.* [9] corresponding to the configuration in Fig. 2.3

L_{wire}, λ	e, λ	L_{ax}, λ	R_{res}, Ω	$\%SR$
0.35	.0133	0.175	21.5	30

- Comparing the experimental results in Table 3.1 with the numerical results in Table 3.2, it is clear that for a shortening ratio of approximately 30%, both configurations [Fig. 2.3 and Fig. 2.4(a)] have the same resonant resistances, R_{res} (approximately 22Ω). Although the resonant resistance data corresponding to a shortening ratio of 30% is unavailable for the configuration in Fig. 2.4(b), from the available data [Table 3.3] it appears that it would be nearly the same as is in the previous two configurations. In conclusion it can be said that for the same shortening ratio all the three configurations have approximately the same resonant resistances.

- If greater shortening (more than 30%) is intended using configuration 2.4(a) or 2.4(b), the results in Table 3.1 and 3.2 show that the resonant resistance would drop to a very low value in comparison to that of a quarter-wave monopole making the matching of the meander antenna to a 50 Ω line very difficult. In that case (for shortening of more than 30%), according to Table 3.1 and Table 3.2, the bandwidth will also be narrow.

- The wire length necessary to make a meander antenna using the configuration in Fig. 2.3 for the same amount of shortening would be less than that for the configuration in Fig. 2.4(a) or 2.4(b). This means that the ohmic losses in

Table 3.3: Experimental and numerical results of Rashed [12] corresponding to the configuration in Fig. 2.4(b); $L_{wire} = 13.5$ cm, $a = 0.4$ mm

$Width, w$ cm	R_{res}, Ω	$\%SR$	$\%BW$	*% Antenna efficiency*, η	f_o, MHz
0.25	14.2	36	3.6	97	962
0.5	7.5	50	2.1	95.1	787
1.0	5	55	1.5	93.2	712

the current carrying wire for the configuration in Fig. 2.3 would be less in comparison to the other two configurations which will eventually increase its efficiency.

In designing the meander antenna using the configuration of Fig. 2.3, the following points were considered –

1. The separation between two horizontal segments should be kept small (separation between segment ab and cd is e in Fig. 3.4(a)) in comparison with the wavelength. If we assume that the currents in those segments have no initial phase difference, then they are exactly out of phase in ab and cd. Now, as $e \ll \lambda$, then according to (2.6), the fields radiated by the horizontal segments would be out of phase and would, therefore, cancel in the far-field. Theoretically, therefore, there should be no cross polarization component present. However, if e is not very small compared to λ, the term e^{-jkr} in (2.6) will introduce some additional phase difference. As a result, the field components due to ab and cd would not be completely out of phase and, therefore, would

not cancel fully in the far-field.

2. In reality, there would always be some cross-polarization component present, because the currents in the horizontal segments would certainly not have the same initial phases. Also the longer the segments [w in Fig. 3.4(a)], the greater would be the fields contributed by them according to (2.6). And as mentioned earlier, the distance between the segments will also introduce some additional phase difference. In conclusion, therefore, it can be said that with increasing separation between two horizontal segments (e) and with increasing horizontal segment length (w), the cross polarization component would increase.

3. However, without the exact picture of the current distribution, the cross polarization component cannot be calculated. But since it would increase with the increase in the segment length and the segment separation, we suggest here that e be kept very small compared with the wavelength. We propose here, that the length of the horizontal segments be kept approximately equal to the length of an infinitesimal dipole ($l = \frac{\lambda}{50}$), the current distribution of which is assumed constant and has no phase difference over the length of the antenna. Since in Fig. 3.4(a) $e/w = 1$, it is suggested that e be kept approximately equal to $\lambda/50$.

The Wire Sinusoidal Antenna

A new class of antennas, the sinusoidal antenna, is proposed here. Such an antenna is shown in Fig.3.4(b). This antenna is similar to the zigzag antenna mentioned earlier except that it does not have the sharp corners of the zigzag. The smooth

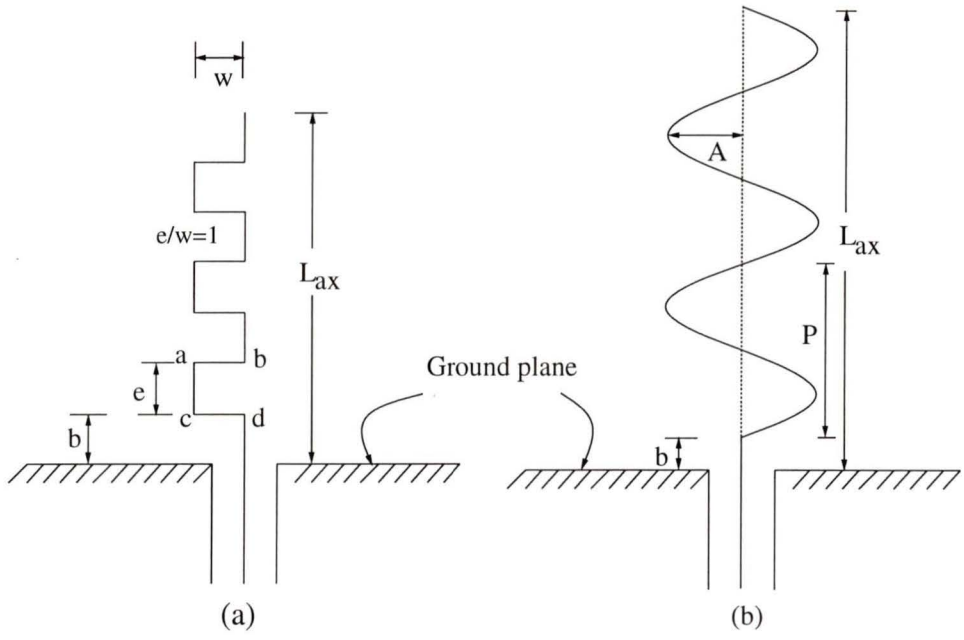

Figure 3.4: (a) A wire meander antenna, (b) a wire sinusoidal antenna

shape of the sinusoid should minimize the current concentration at the corners of the zigzag and is expected to produce better characteristics than the zigzag.

The design parameters and the radiation characteristics of the monopole version of the zigzag antennas investigated by Nakano and his colleagues [9] are shown in Table 3.4. According to their results within the design limits of Table 3.4, the antenna radiation pattern is similar to that of a straight antenna and the cross-polarization component is also minimum.

The main design problem, however, is related to the radiation resistance. From Table 3.4 it is evident that unlimited shortening can not be achieved because with increased shortening the radiation resistance would decrease sharply. Although a 24 or 34 percent or even more shortening can be achieved by increasing the ampli-

Table 3.4: Design data and radiation characteristics of the monopole version of the zigzag antenna investigated by Nakano *et al.* [9]

parameters	*Case I*	*Case II*	*Case III*
Period P, λ	0.0749	0.0542	0.0412
Amplitude A, λ	0.009	0.0157	0.018
Number of periods	3	3.5	4
% Shortening ratio, SR	10	24	34
Radiation resistance, Ω	32.5	23	18.5

tude and decreasing the period, the result would be even lower radiation resistance resulting in a poor match for a 50 Ω feeding coaxial cable.

Because of similar geometry, the design limits of the zigzag will also be applicable to the sinusoidal antenna. To discuss the cross-polarization constraints of a sinusoidal antenna let us consider the equivalent field diagram of a zigzag antenna in Fig. 3.5. It has been assumed that the zigzag antenna generates the equivalent horizontal and vertical fields shown by the solid lines in Fig. 3.5. Let us also assume that the equivalent vertical and horizontal fields shown in Fig. 3.5 are generated by exactly similar vertical and horizontal segments.

Similar to the meander antenna case to ensure minimum cross-polarization it is suggested here that –

1. The distance between two equivalent horizontal segment ($P/4$) be kept very

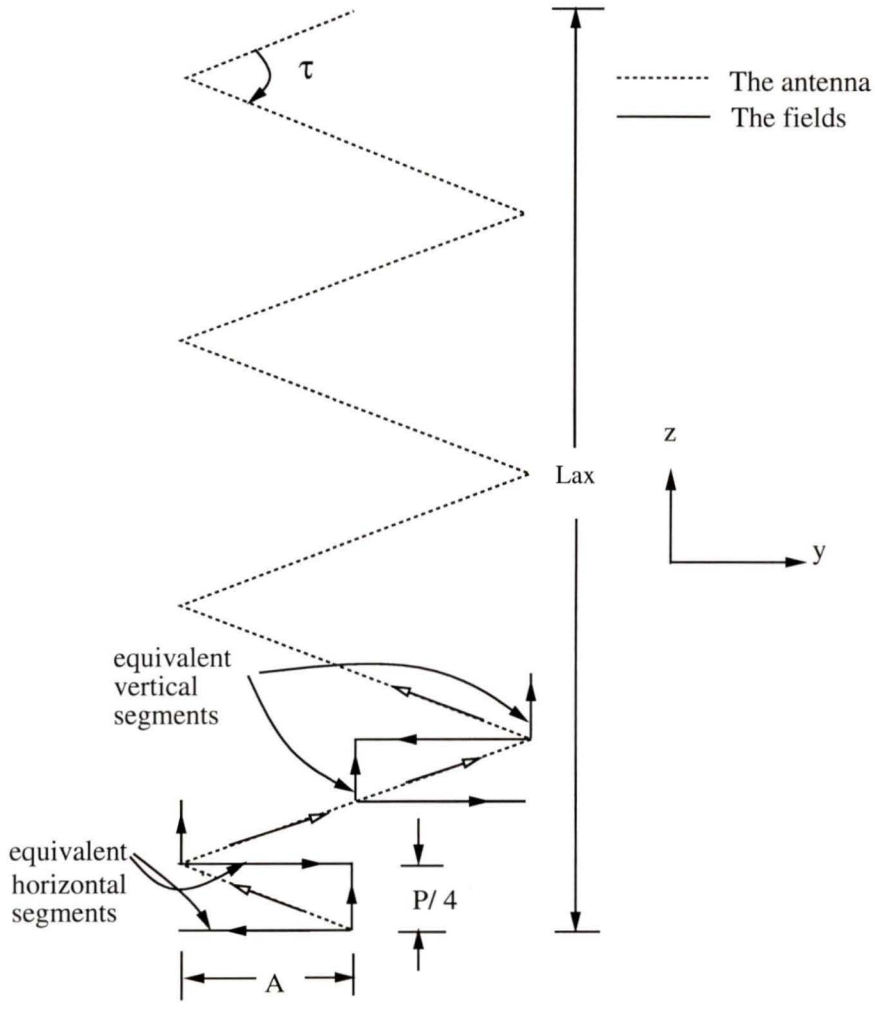

Figure 3.5: The equivalent field diagram of a zigzag antenna

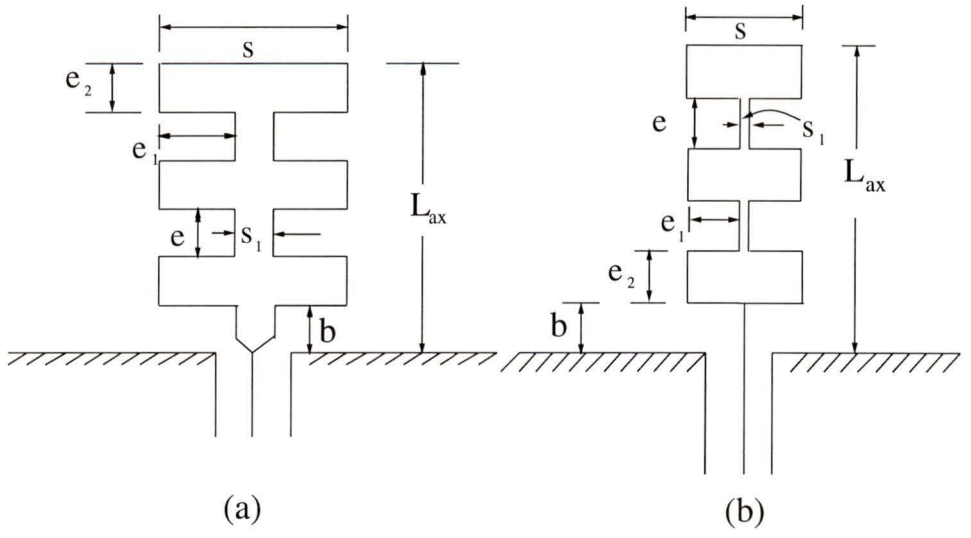

Figure 3.6: (a) The dual meander antenna of Wong *et al.* [10], (b) the dual meander antenna proposed here

small compared to the excitation wavelength.

2. The length of each equivalent horizontal segment (A) be kept approximately equal to the length of an infinitesimal dipole ($\lambda/50$).

The wire dual meander antenna

The dual meander antenna was first proposed and investigated by Wong *et al.* [10]. They designed a dual meander antenna operating at a frequency of 400 MHz which is shown in Fig. 3.6(a). The dual meander antenna we designed is shown in Fig. 3.6(b). The parameters of these two antennas are compared in Table 3.5.

It has been proposed during discussing the design considerations of the meander antenna that to ensure minimum cross-polarization, the distance between two hor-

Table 3.5: Comparison between the design parameters of the dual meander antenna of Wong *et al.* [10] and those of the dual meander antenna proposed here

Antenna Type	e, λ	e_1, λ	e_2, λ	l_{wire}, λ	L_{ax}, λ	$\frac{l}{d}$
Design of Wong et al.	0.0508	0.03386	0.0677	0.93133	0.18	87.16
Our design	0.0234	0.0234	0.0234	0.76244	0.19	32.8

izontal segments and the length of each horizontal segment [e in Fig. 3.4(b) since $e = e_1 = e_2$] be kept very small compared to λ. Considering these points once again for the dual meander configuration, we have kept the horizontal segment length and the distance between two consecutive horizontal segments [see Fig. 3.6(b) and Table 3.5] the same and very small compared to λ. It is relevant to mention that the dimensions in our design are smaller than the dimensions in the design of Wong *et al.* [10].

3.2.2 Printed Bent Antennas

Since the wavelength in the dielectric is shorter than the free space wavelength, any bent antenna etched on a dielectric substrate will certainly be shorter than the wire bent antenna when the design variables are same. And also since it is difficult to bend a wire exactly like a meander or a sinusoid, we propose here that bent configurations be drawn using Autocad with exact scaling and then etched on a dielectric substrate using printed circuit technology.

We consider bent antennas to be etched on fiberglass dielectric substrate with a dielectric constant, ϵ_r of 4.2. The dielectric is assumed to be lossless, and a very thin substrate (thickness, t = 1.5 mm) is suggested so that it does not affect the standard monopole radiation pattern. The antenna configuration will be etched on one side of the substrate and the copper from the other side will be etched off. The width of the substrate is 2.0 cm.

Printed Meander Antenna

Since we have proposed that the segment length of a wire meander antenna [e in Fig. 3.4(a)] be kept very small compared to λ to minimize cross-polarization, and since the wavelength on a substrate is shorter than the free space wavelength, we propose here that the segment length, ϵ for the printed meander antenna be further reduced than the wire meander antenna.

Printed Sinusoidal Antenna

We propose here that after the wire sinusoidal antenna being investigated, an optimum design will be considered which will provide the adequate bandwidth and the best possible shortening for application in PCN handset. Applying the same reasoning as the printed meander antenna case we propose here that A and P for the printed sinusoidal antenna be kept smaller than those parameters for the wire sinusoidal antenna.

3.3 Design of a Broadband Sleeve Antenna

Let us consider the sleeve antenna configuration in Fig. 3.7 and the equivalent circuit in Fig. 2.6. Design of a sleeve antenna at a single frequency can proceed either by assuming a sleeve length or a sleeve diameter. To assume the sleeve diameter approach is better because the length can be decreased or increased easily unlike the changing of the sleeve diameter. Thus if a sleeve diameter is fixed, the characteristic impedance of the transmission line made by the sleeve and the antenna can be calculated as [38]

$$Z_0 = \frac{138}{\sqrt{\epsilon}} \log_{10} \frac{b}{a} \tag{3.3}$$

where, b is the sleeve diameter (inner diameter of the outer conductor of the transmission line section), a is the diameter of the antenna and ϵ is the dielectric constant of the medium inside the sleeve.

Now, let us assume that the monopole antenna has an input impedance of R_o, at resonance (f_o). Referring to the equivalent circuit in Fig. 2.6,

$$Z_L = -\frac{jX_C R}{R - jX_C} \tag{3.4}$$

where, Z_L is the combined impedance before the transmission line section and R is defined by (2.28). Now the input impedance at the base of the antenna [terminals m-n in Fig. 2.6]

$$Z_{in} = Z_0 \frac{Z_L + jZ_0 \tan\theta}{Z_0 + jZ_L \tan\theta} \tag{3.5}$$

where, θ is defined by (2.29). Assuming that the feeding coaxial cable has a characteristic impedance of 50 Ω, for perfect match at f_o,

$$50 = Z_0 \frac{Z_L + jZ_0 \tan\theta}{Z_0 + jZ_L \tan\theta} \tag{3.6}$$

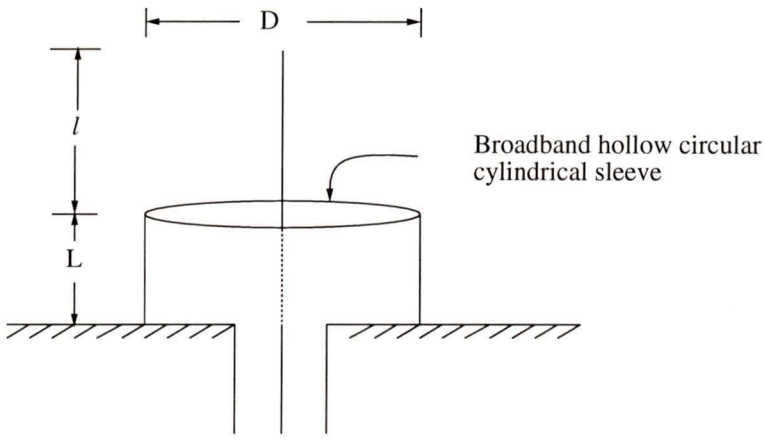

Figure 3.7: A wire monopole antenna with hollow circular cylindrical sleeve

The unknowns in (3.6) are X_C and L, the capacitive reactance and the length of the line. Equating the real and imaginary parts from (3.6),

$$50(Z_o R + R X_C \tan\theta) = Z_o^2 X_C \tan\theta \tag{3.7}$$

$$-50 Z_o X_C = Z_o^2 R \tan\theta - Z_o X_C R \tag{3.8}$$

Now, from (3.8),

$$X_C = \frac{Z_o^2 R \tan\theta}{Z_o R - 50 Z_o} \tag{3.9}$$

Substituting the value of X_C in (3.7), and solving for Z_o gives,

$$Z_o = \sqrt{\frac{50(R - 50 + R\tan^2\theta)}{\tan^2\theta}} \tag{3.10}$$

Using (2.28) and (3.10), the value of θ can be found out numerically. And the evaluation of θ would lead to the evaluation of the sleeve length L because $\theta = \frac{2\pi L}{\lambda}$.

Burberry [39] has presented a summary of different types of sleeve antennas. The broadband sleeve configuration described by him has a length to diameter ratio of 2.5 : 1 and after the sleeve the antenna is extended with the sleeve diameter because

thicker antennas produce less sidelobes [29]. Following this design we considered a sleeve diameter of 3.25 cm because a monopole antenna with a wire diameter of 2.5 mm and operating at a center frequency of 880 MHz has a length of 8.2 cm [see section 3.1.2]. Now, Z_o can be calculated using (3.3),

$$Z_o = \frac{138}{\sqrt{\epsilon}} \log_{10} \frac{32.5}{2.5} = 153.72\ \Omega \tag{3.11}$$

where, $\epsilon = 1$. The calculated input impedance of the monopole antenna at resonance [see from section 3.1.2] is 33 Ω.

For $Z_o = 153.72\ \Omega$, and $R_o = 33\,\Omega$, evaluating (3.10) gives, $\theta = 1.29$ rad. Thus, the sleeve length is 7.1 cm. A straight monopole antenna with a wire diameter of 2.5 mm would only be 8.2 cm long as mentioned in section 3.2. In comparison to the monopole, the sleeve is only 1.1 cm shorter. However, this design is done at a single frequency, f_o and therefore is not a complete one. To do a complete design (over a frequency range of 2 : 1 or 3 : 1 etc.) using analytical methods, the input impedance of the sleeve antenna at all frequencies is to be calculted which is indeed a formidable task.

Therefore, we propose here the experimental parametric study of the sleeve antenna as was done before by Poggio *et al.* [29] and King *et al.* [31]. We consider the monopole antenna of 8.2 cm with a sleeve with diameter 3.25 cm and length 7.1 cm. As it is well known that the hollow circular cylindrical sleeve can be substituted by one or more open posts [31], it is proposed here that two matching posts be connected to the ground plane at the two extremes of the sleeve diameter.

The matching posts will be made from the same wire which was used to make the antenna and will be called 'sleeves' instead of matching posts from now on. In

fact the 'sleeves' connected to the ground plane is nothing but the simulation of a hollow circular cylindrical sleeve if a large number of rods are used and if the same sleeve spacing is maintained.

The experimental design will proceed with the aforementioned sleeve length and diameter and the sleeve would be trimmed at regular intervals. The optimized sleeve length will thus be determined by observing the VSWR of the antenna.

Chapter 4

Experimental Objectives and Procedures

4.1 Experimental Objectives

As mentioned in Chapter 1 the objective of this thesis was to explore and develop small wideband antennas for the application in PCN handsets. It has also been mentioned that to accomplish this objective linear antennas have been bent according to some specific geometric configurations [9], [10].

Although, finally, the handset antenna is to be mounted on a small conducting box, the investigation of bent antennas were kept limited to 'antennas on a large ground plane'. The reasons for doing this are as follows -

- To compare the characteristics of the new bent antennas to those investigated by other researchers, because their investigation of bent antennas involves either monopoles on large ground planes or dipoles.

- With the reduction of ground plane size, the radiation pattern or the input impedance of any monopole antenna will change [25]. The main disadvantage of mounting the antenna on a small box will be the tilting of the radiation pattern and the reduction in the VSWR bandwidth. The problem of comparatively high VSWR can be solved by designing matching circuits and by implementing those for the specific antenna. The direction of maximum radiation would be changed from $\theta = 90°$ to a value less than that when the size of the ground plane is reduced [25].

- Designing of matching circuits to improve the VSWR bandwidth for a specific antenna on a small conducting box and investigating its radiation pattern is left for future investigation.

4.2 Experimental Procedures

Initially, experiments were conducted using an HP 8757A scalar network analyzer (SNA). Since the phase of the input reflection coefficient cannot be measured by a scalar network analyzer, and since the input impedance of an antenna cannot be measured without it (see equation 2.15), later on an HP 8720B vector network analyzer (VNA) was used to investigate the input impedance characteristics of various antennas.

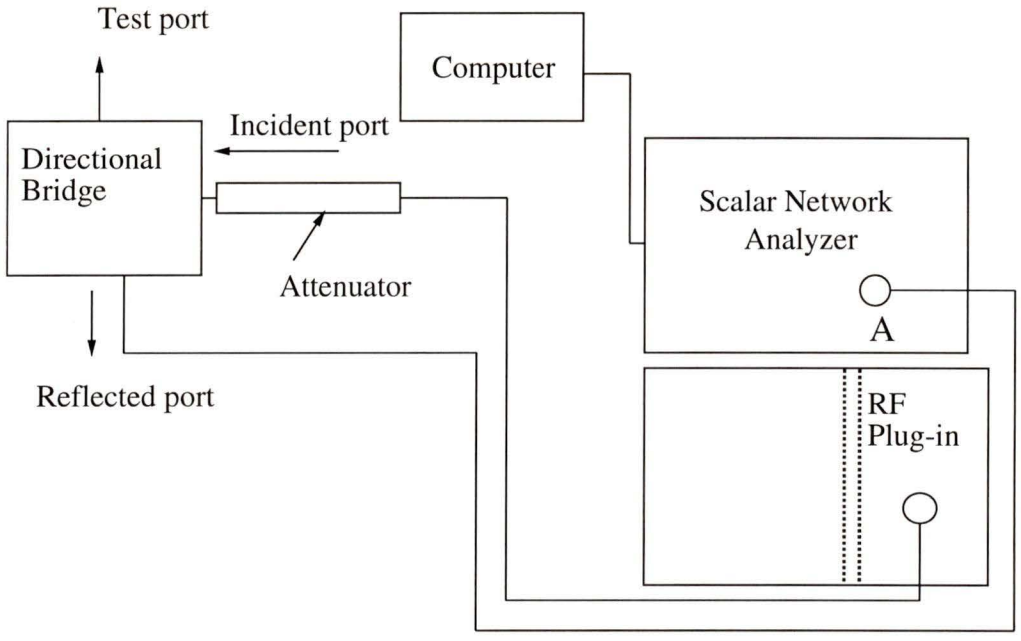

Figure 4.1: Experimental arrangement in block diagrams

The experimental arrangement is shown in Fig. 4.1 in block diagrams. According to this figure the directional bridge has three ports:

The Incident Port connected to the HP 8359A RF Plug-In through a calibrated 10 dB attenuator,

The Reflected Port connected to the SNA and

The Test Port connected to the antenna.

The connection scheme of the antenna with its associated connectors and the ground plane is shown in Fig. 4.2. Each antenna was soldered to the center pin of an N type panel mounted female connector [Fig. 4.3(b)]. To make the antenna work as a monopole the outer conductor of the connector was connected to a ground

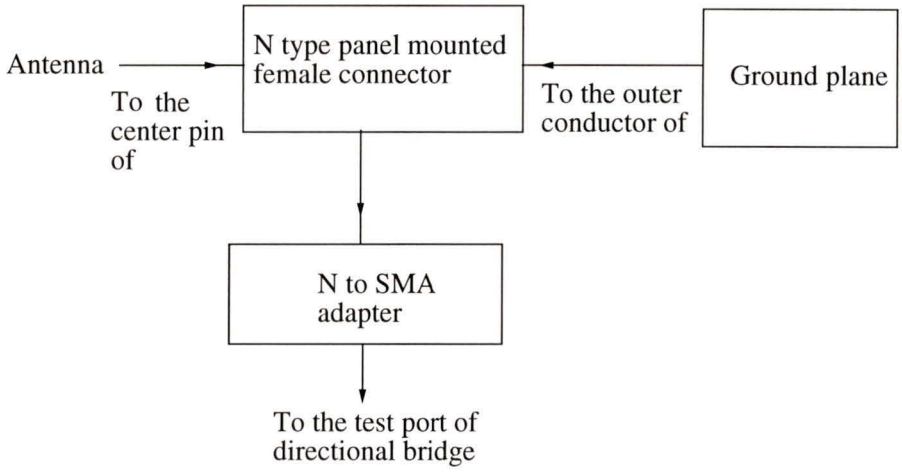

Figure 4.2: The antenna connection scheme in block diagrams

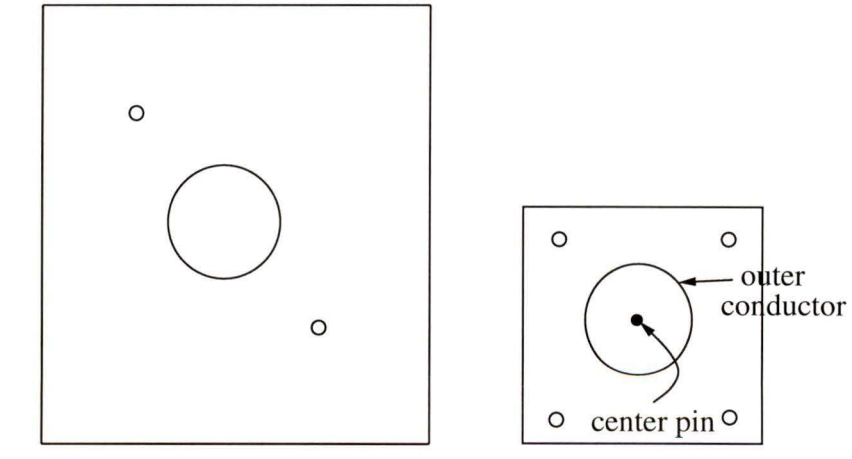

(a) Top view of the ground plane

(b) Top view of the N type connector

Figure 4.3: The ground plane and the connectors

plane of dimension 89 cm $\times$84 cm $\times$1 mm [Fig. 4.3(a) and 4.3(b)]. Each side of the ground plane has an approximate length of 2.46λ.

To perform measurements the frequency range was selected first and then the SNA was calibrated using a standard short and a standard open. The calibration was saved in the network analyzer memory. Each antenna was initially made longer. Then observing the VSWR on the SNA screen the antenna was trimmed in order to operate it at a specific center frequency.

The network analyzer was also connected to a computer by the GPIB bus to transfer the measurement data from the SNA to the computer. The SNA measures the magnitude of the reflection coefficient ($|\Gamma|$) in return loss ($return\ loss = -20\ \log_{10}\ |\Gamma|$) and in VSWR format. The measured data were saved in separate files for separate antennas. Data were saved in three columns: the first column was for frequency, the second column was for VSWR and the third column was for return loss. The data files were then used to present the results in graphical and in tabular forms.

The antenna connection scheme with the VNA was similar to that in Fig 4.2 except that there was no directional bridge and the N to SMA adapter was directly connected to port 1 of the VNA by a 50 Ω coaxial cable. Similarly to the SNA, the VNA was also calibrated before measurement and the calibration was saved in register 3. For accurate phase measurements the length between the calibration point (the end point of the feed line) and the antenna input was taken into consideration by establishing a short circuit between the N type connector and the ground plane by using an aluminium foil. This length compensation was performed by changing the electrical delay until a smooth phase frequency response was observed. The

VNA measures both the magnitude and the phase of the reflection coefficient, Γ. Similarly to the SNA the measured data were transferred to the computer.

Chapter 5

Experimental Results

5.1 Bent Wire Antennas

Experimental investigations of wire antennas were conducted on two different wires with diameters 2.5 mm and 0.65 mm. The results found from experiments are presented in two different subsections. The heading 'Thick Bent Antennas' represents antennas made from the wire with a diameter of 2.5 mm, whereas the other heading 'Thin Bent Antennas' represents antennas made from the wire with a diameter of 0.65 mm.

5.1.1 Thick Bent Antennas

Experiments were conducted on a meander and a sinusoidal antenna. To compare the characteristics of these antennas with a straight antenna, the latter was made

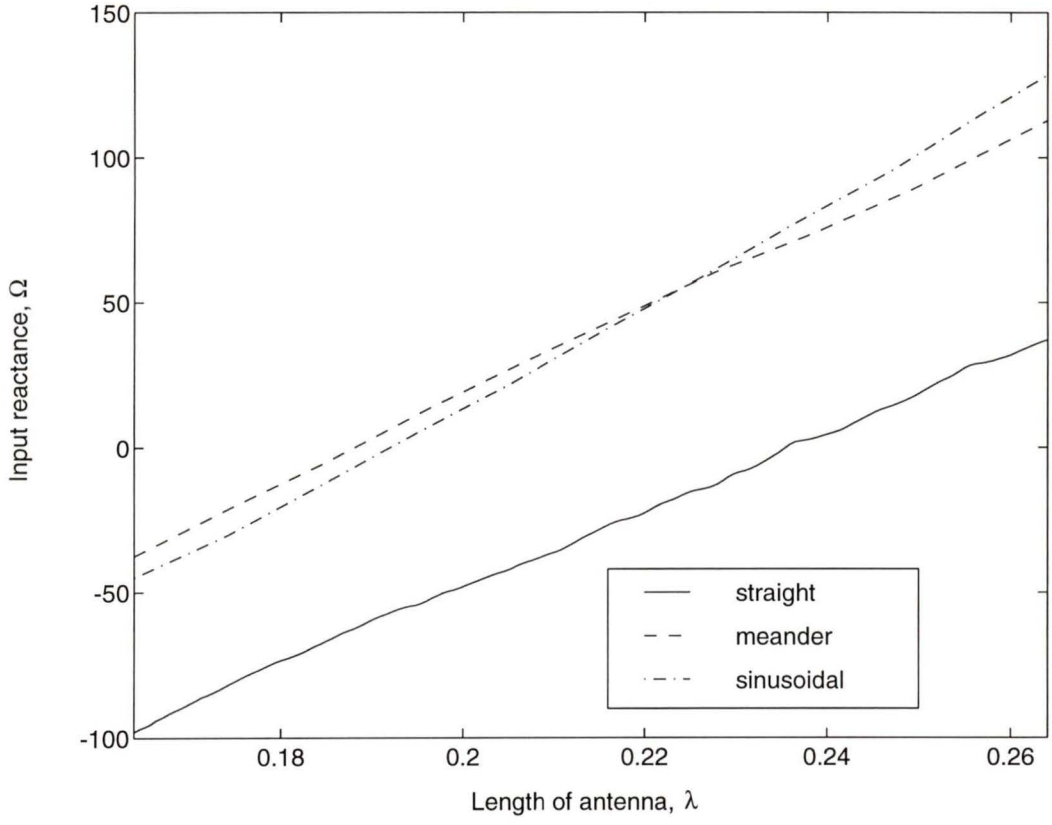

Figure 5.1: Input reactance characteristics of wire antennas

from the same wire and then measured. The segment length e of the meander antenna [Fig. 3.4(a)], and the period P and amplitude A of the sinusoidal [Fig. 3.4(b)] antenna are listed in Table 5.1.

All the three above mentioned antennas were operated at a center frequency of 880 MHz. It has been found that the meander and the sinusoidal antennas were 6.78 cm and 6.8 cm long in comparison to the straight antenna of 8.2 cm. The shortening ratios of the two bent antennas are listed in Table 5.2.

To present the phenomenon of shortening in a clear context, the measured input

Table 5.1: Dimensions of the meander and the sinusoidal antenna

Antenna Dimensions	*Meander*	*Sinusoidal*
Segment length, e cm	1.25	–
Period, P cm	–	1.7
Amplitude, A cm	–	0.7
Base length, b cm	1.6	1.6

reactances of the meander, the sinusoidal, and the straight antenna are plotted against antenna lengths normalized to the excitation wavelengths in Fig. 5.1. It is clear from Fig. 5.1 that the bent antennas cross the zero reactance axis (or resonating) with a shorter length than the straight antenna.

The VSWR frequency responses of the antennas under consideration are shown in Fig. 5.2. From these results the respective operating frequency ranges and the minimum VSWR's are determined and listed in Table 5.2. The bandwidths of these antennas were then calculated using the definition presented in section 1.1.1 and are listed in Table 5.2.

From the VSWR response shown in Fig. 5.2 and from the results in Table 5.2 two important points are noticeable. These are -

- The sinusoidal antenna is more wideband than the meander when they have very nearly the same shortening ratio.
- The minimum VSWR for the sinusoidal antenna is also lower than the mean-

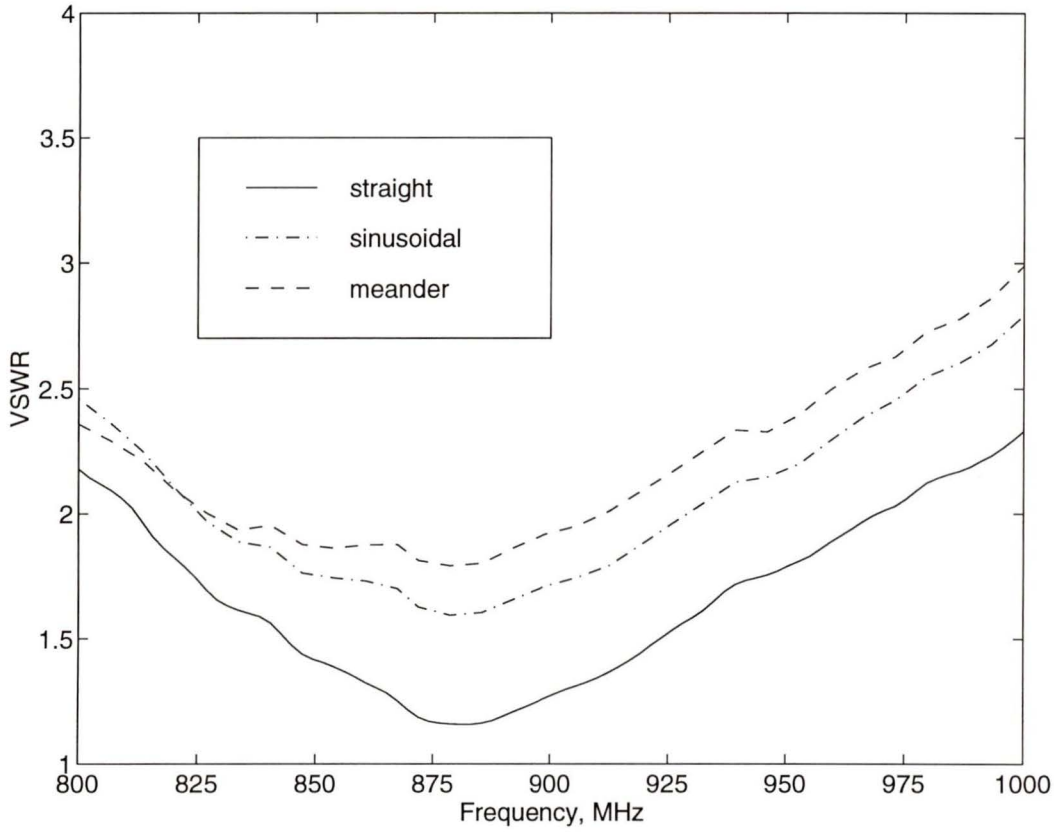

Figure 5.2: VSWR vs frequency characteristics of wire antennas

Table 5.2: Characteristics of the meander and the sinusoidal antenna

Antenna characteristics	*straight*	*Meander*	*Sinusoidal*
% SR	–	17.32	17.07
Operating frequency range	812 – 970 MHz	828 – 912 MHz	827 – 928
% BW	17.95	9.55	11.48
Minimum VSWR	1.2	1.8	1.6

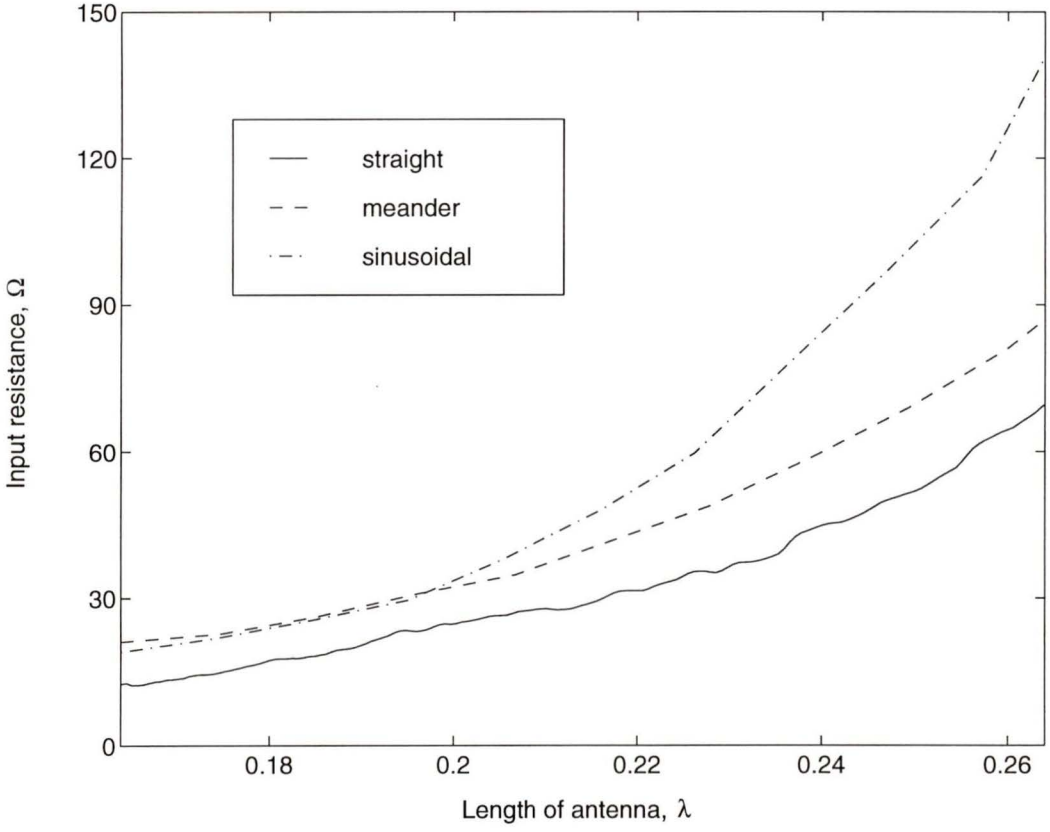

Figure 5.3: Input resistance characteristics of wire antennas

der.

The narrowing of bandwidth and higher minimum VSWR behavior of bent antennas can be understood from the resonant resistance, R_{res} behavior of those antennas. The resonant lengths for the straight, the meander and the sinusoidal antenna from Fig. 5.1 are 0.233λ, 0.187λ, and 0.192λ respectively. The corresponding R_{res} for these antennas can be found out from the input resistance characteristics curves shown in Fig. 5.3.

The resonant resistances, R_{res} for the straight, the meander and the sinusoidal

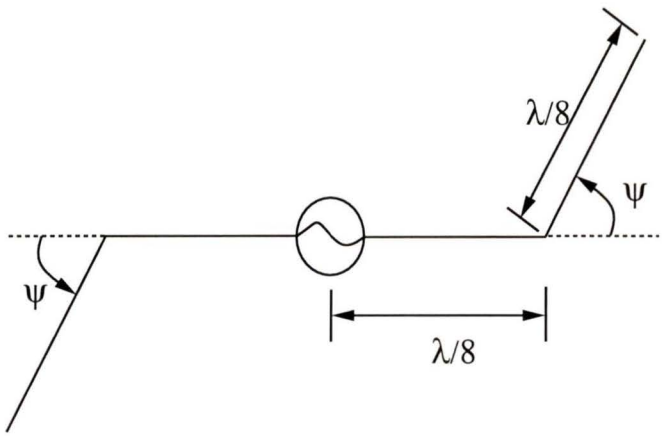

Figure 5.4: Bent dipole antenna of Nakano *et al.* [41]

antenna from Fig. 5.3 are 36 Ω, 25 Ω, and 28 Ω. Since R_{res} values for the bent antennas are lower than a straight monopole, impedance matching of those antennas with a 50 Ω line is difficult. This difficulty is confirmed by the fact that the VSWR curves of the bent antennas have moved up and therefore, the antennas have become narrowband.

The reason why R_{res} values for bent antennas are lower can be explained by drawing an analogy with the work of Nakano *et al.* [41] on a center-fed bent dipole. The antenna configuration is shown in Fig. 5.4. It has been reported that with the increase in the bending angle Ψ, the amplitude of antenna current, I_o increases. This increase begins as Ψ exceeds 0° and continues until it is 90°. The current decreases sharply as Ψ exceeds 90°.

Similarly it can be said that the amplitude of current increases when the antenna is made as a sinusoid or meander. Now it is well known that the input power and

the input resistance of an antenna are related as [7]

$$P_{in} = \frac{1}{2}|I_{in}|^2 R_{in} \tag{5.1}$$

For a constant input power, P_{in}, if $|I_{in}|$ increases that will simply mean that R_{in} will decrease meaning that R_{res} will also decrease. Therefore, the R_{res} values for bent antennas are certainly lower than that of a straight antenna.

5.1.2 Thin Bent Antennas

The Sinusoidal Antenna

Let us consider the sinusoidal antenna configuration of Fig. 3.4(b) where the design variables are the period P and the amplitude A. To investigate the characteristics of this configuration several such antennas were made by varying the design parameters. The antennas that were made fall into three groups:

Group I when P is constant and A is variable: The measured VSWR responses of these group of antennnas are shown in Fig. 5.5. Each curve represents the VSWR frequency characteristics of the sinusoidal antenna when amplitude A is the parameter. Characteristics such as the shortening ratio, the bandwidth, the minimum VSWR etc. are listed in Table 5.3.

From Table 5.3 it is clear that to achieve larger shortening, A has to increase. But on the other hand according to Fig. 5.5 with increasing A the VSWR curves are found to be moving up meaning that the antenna bandwidth is becoming narrower. Therefore, to maintain a certain amount of bandwidth the shortening will certainly have to be limited.

For example, for a shortening of 24.71%, the bandwidth of the antenna is 5.26% [see Table 5.3]. For greater amounts of shortening, A has to be increased for which the VSWR curve will move further up. Now, if the shortening exceeds 30%, the VSWR curve will move above the 2 : 1 line meaning the antenna will have zero bandwidth.

Group II when A is constant and P is variable: The VSWR vs frequency characteristics of these group of antennas are shown in Fig. 5.6. The shortening ratio, bandwidth and other important parameters are listed in Table 5.4. According to the characteristics in Fig. 5.6 it is clear that with a constant A the VSWR curve of the sinusoidal antenna moves up when P decreases.

But the results in Table 5.4 confirm that without decreasing P the shortening ratios of these antennas cannot be increased. Experimental results with these group of antennas again confirm that with a shortening ratio of more than 30%, the bandwidth is zero.

Group III when both P and A are variable: This group of antennas were made by varying both the period and the amplitude. For this group of antennas the results are presented in Table 5.5. Similar to the previous two cases here it is also seen that as the shortening ratio increases beyond 30%, the bandwidth becomes zero. However, with comparatively high VSWR (around 2.95) the shortening ratio can be as high as 44.71%.

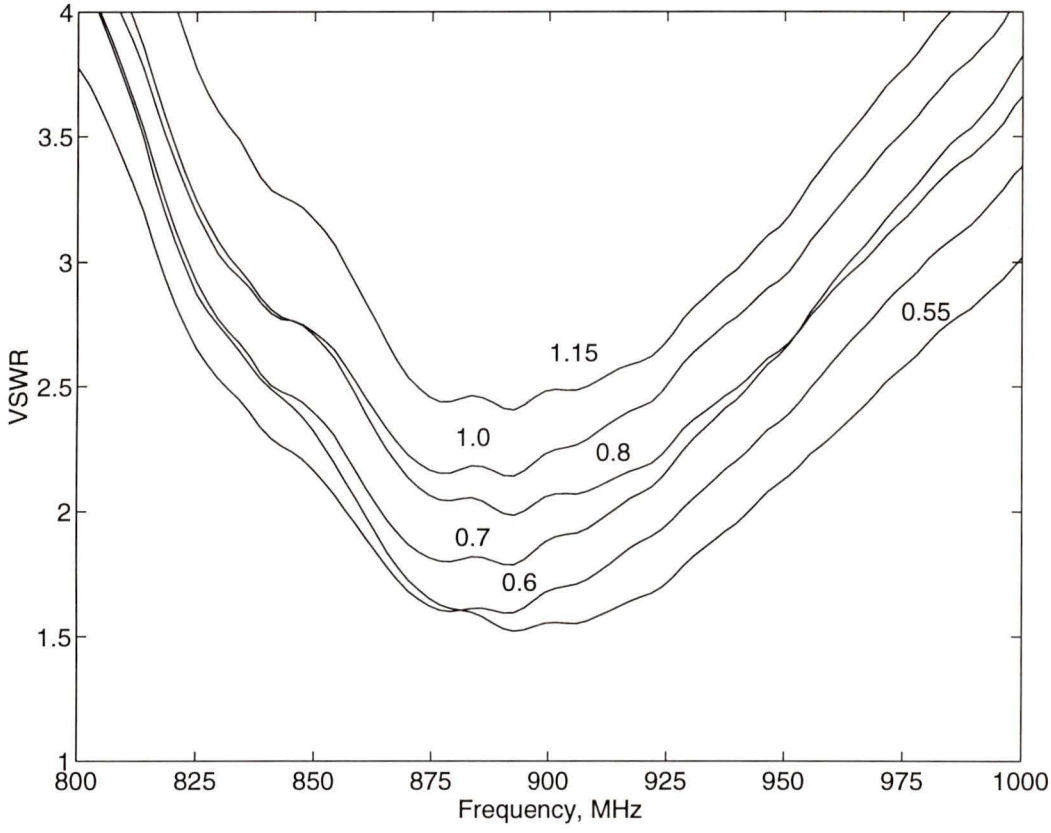

Figure 5.5: VSWR vs frequency characteristics of wire sinusoidal antennas. Period, $P = 1.9$ cm; amplitude, A (cm) is the parameter.

Table 5.3: Wire sinusoidal antenna characteristics; period P is 1.9 cm and wire diameter is 0.65 mm. Amplitude A (cm) is the variable

Parameters	Case I	Case II	Case III	Case IV	Case V	Case VI
A, cm	0.55	0.6	0.7	0.8	1.0	1.15
P/A	3.45	3.17	2.71	2.38	1.9	1.65
L_{ax}, cm	6.95	6.8	6.4	5.95	5.4	5.2
Minimum VSWR	1.51	1.59	1.79	1.99	2.14	2.41
% BW	9.3	8.07	5.26	.34	0	0
% SR	18.23	20	24.71	30	36.47	38.82

Table 5.4: Wire sinusoidal antenna characteristics; amplitude A is 0.6 cm and wire diameter is 0.65 mm. Period, P (cm) is the variable

Parameters	Case I	Case II	Case III	Case IV
P, cm	1.9	1.5	1.3	1.0
P/A	3.17	2.5	2.17	1.67
L_{ax}, cm	6.8	6.1	5.8	5.2
Minimum VSWR	1.59	1.94	2.17	2.52
% BW	8.07	3	0	0
% SR	20	28.23	31.76	38.82

Table 5.5: Wire sinusoidal antenna characteristics; amplitude is A (cm) and period is P (cm). Both are variable. Wire diameter=0.65 mm

Parameters	Case I	Case II	Case III
A, cm	0.4	0.85	1.0
P, cm	1.3	1.7	1.1
P/A	3.25	2	1.1
L_{ax}, cm	6.8	5.45	4.7
Minimum VSWR	1.53	2.16	2.95
% BW	8.99	0	0
% SR	20	35.88	44.71

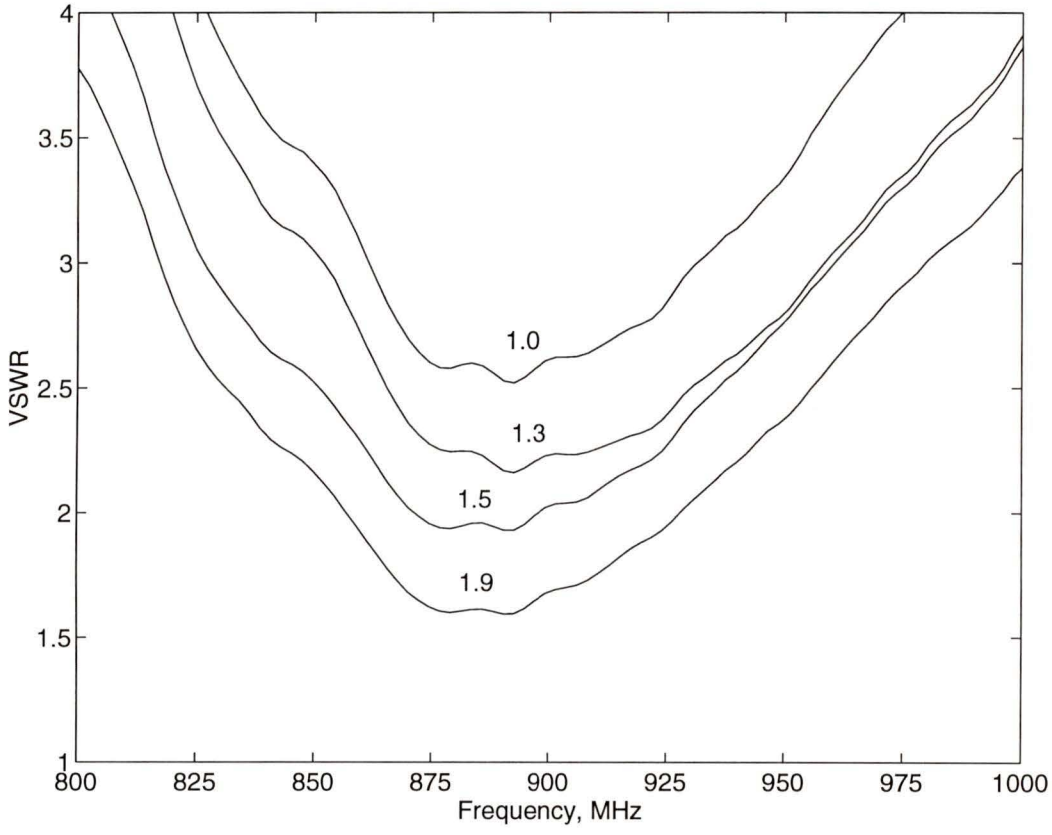

Figure 5.6: VSWR vs frequency characteristics of wire sinusoidal antennas. Amplitude, $A = 0.6$ cm, Period, P (cm) is the parameter.

The Meander Antenna

To investigate the characteristics of the meander configuration corresponding to Fig. 3.4(a), several such antennas were made using the same wire that was used to make the sinusoidal antennas. Since the only design parameter for the meander configuration is the segment length e, the experimental results are plotted in Fig. 5.7 with e as the parameter.

From these results, it is clear that with the increase in e, the shortening ratio increases but at the same time the antenna bandwidth narrows. The bandwidth, shortening ratio, minimum VSWR etc. of these meander antennas are listed in Table 5.6. Comparing these results with those found for the sinusoidal antennas [see Table 5.3, 5.4 and 5.5] one can clearly see that the sinusoidal antenna has wider bandwidth when the shortening ratios of both the antennas are same.

This has also been demonstrated in Fig. 5.8 where the VSWR frequency responses of both these antenna configurations (the meander and the sinusoidal) are plotted with percent shortening ratio as a parameter. It is clear from Fig. 5.8 that for any amount of shortening ratio the VSWR curve for the sinusoidal antenna is below that of the meander.

5.1.3 Summary

The shortening effect of bent antennas has been explained from their input reactance behavior. The narrowing of bandwidths in bent antennas has also been explained. The results for the three groups of sinusoidal antennas investigated show that limit-

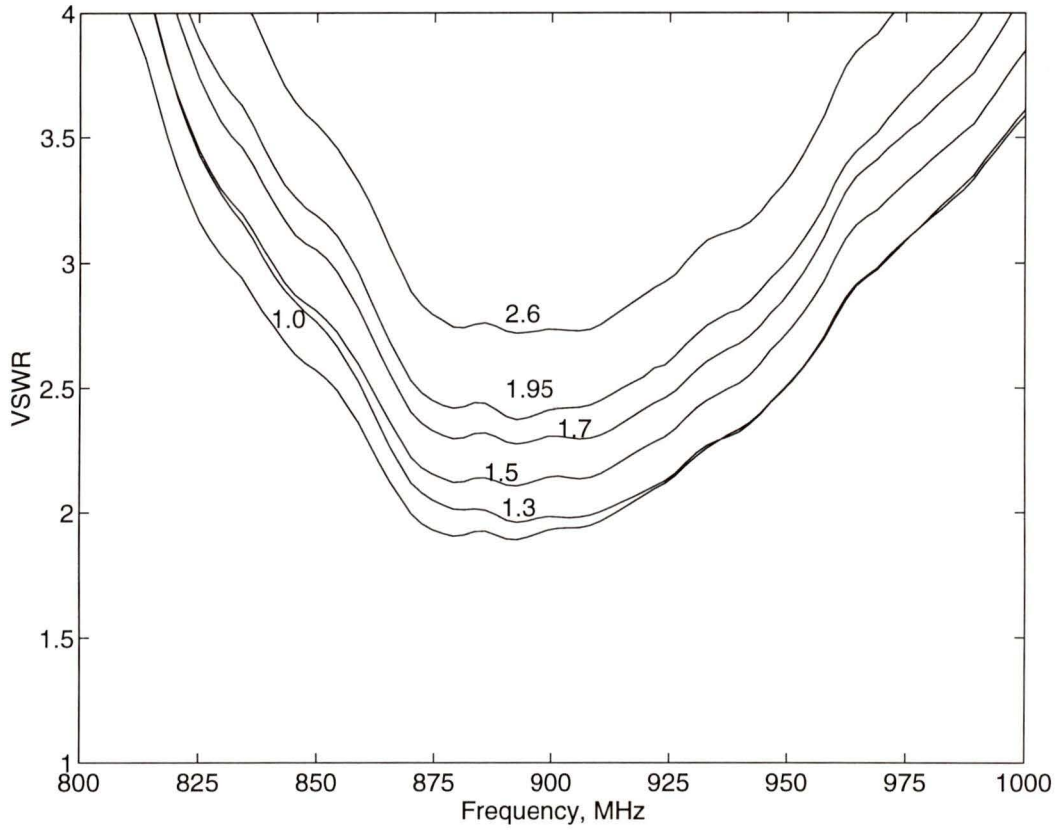

Figure 5.7: VSWR vs frequency characteristics of wire meander antennas where segment length e (cm) is the parameter

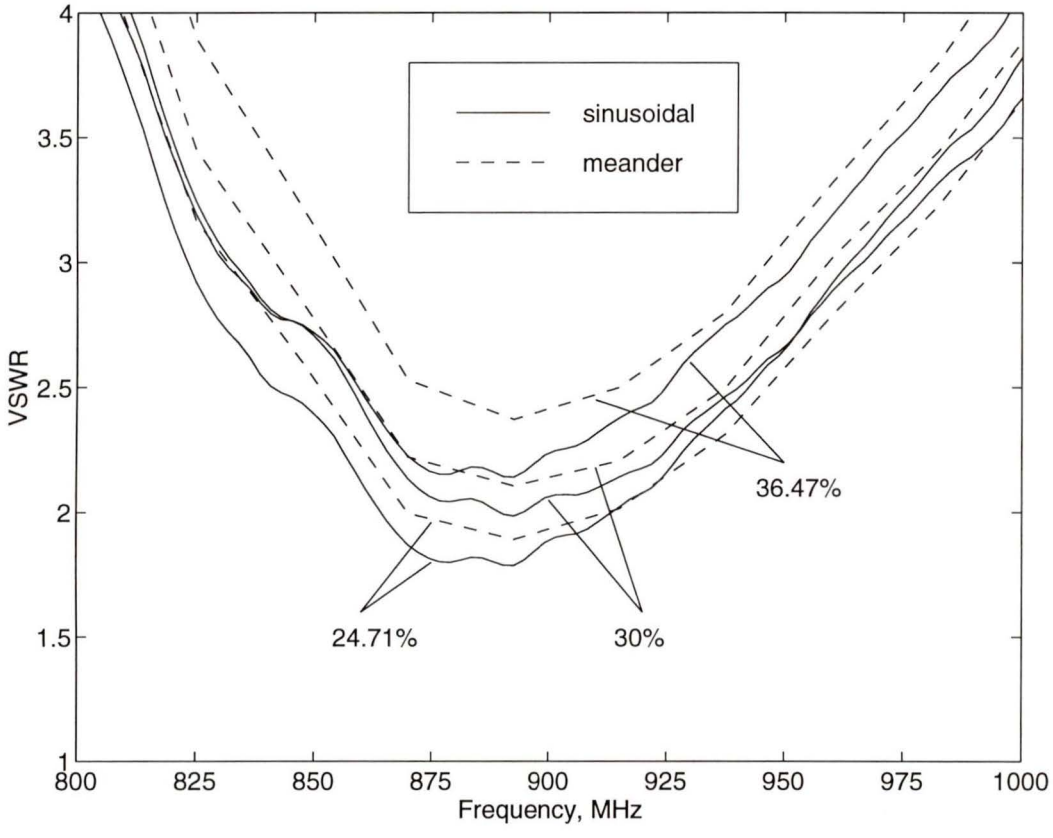

Figure 5.8: Comparison of VSWR frequency characteristics between the meander and the sinusoidal antenna where percent shortening ratio is the parameter

Table 5.6: Wire meander antenna characteristics; wire diameter=0.65 mm, segment length e (cm) is the variable

Parameters	Case I	Case II	Case III	Case IV	Case V	Case VI
e, cm	1.0	1.3	1.55	1.7	1.95	2.6
L_{ax}, cm	6.4	6.15	5.95	5.95	5.4	5.3
Minimum VSWR	1.90	1.94	2.11	2.29	2.37	2.71
% BW	4.71	2.24	0	0	0	0
% SR	24.71	27.65	30	30	36.47	37.65

ted amount of shortening can be achieved if the antenna is expected to operate below the VSWR 2.0.

Experimental results for the meander configuration are also presented in graphical and in tabular form. The bandwidth and shortening ratio characteristics of the meander and the sinusoidal configurations are compared.

5.2 Printed Bent Antennas

5.2.1 Antenna Characteristics

To provide further shortening bent antennas were etched on some suitable dielectric substrates. To accomplish this objective a sinusoidal and a meander antenna were

Table 5.7: Dimensions of the printed meander and the printed sinusoidal antenna

Antenna Dimensions	*Meander*	*Sinusoidal*
Segment length, e cm	0.8	–
Period, P cm	–	1.75
Amplitude, A cm	–	0.625
Base length, b cm	1.13	1.13

etched on a fiberglass substrate with $\epsilon_r = 4.2$. According to the results in Table 5.3 for wire sinusoidal antennas, if P/A is considered to be the variable, then it can be seen that between the P/A ratio of 3.1 to 2.71 a sinusoidal antenna provides a shortening ratio of 20 to 24.71% while the bandwidth varies between 8.07% to 5.26%.

We considered a sinusoidal antenna with a P/A ratio of 2.8 ($P = 1.75$ cm and $A = 0.625$ cm). It was expected that the antenna should have a bandwidth between 8.01 to 5.26% and the shortening ratio should be higher than the wire sinusoidal antenna of the same dimension. For comparison a meander antenna [Fig. 3.4(a)] was also etched on the same substrate. The dimensions of these two antennas are listed in Table 5.7.

The VSWR vs frequency characteristics of the printed meander and the sinusoidal antenna are shown in Fig. 5.9. The experimentally determined characteristics of these two antennas are listed in Table 5.8.

Table 5.8: Characteristics of the printed meander and the printed sinusoidal antenna.

Antenna characteristics	*Meander*	*Sinusoidal*
% SR	29.64	29.64
Operating frequency range, MHz	862 – 915 MHz	862 – 928
% BW	6.02	7.42
Minimum VSWR	1.83	1.770

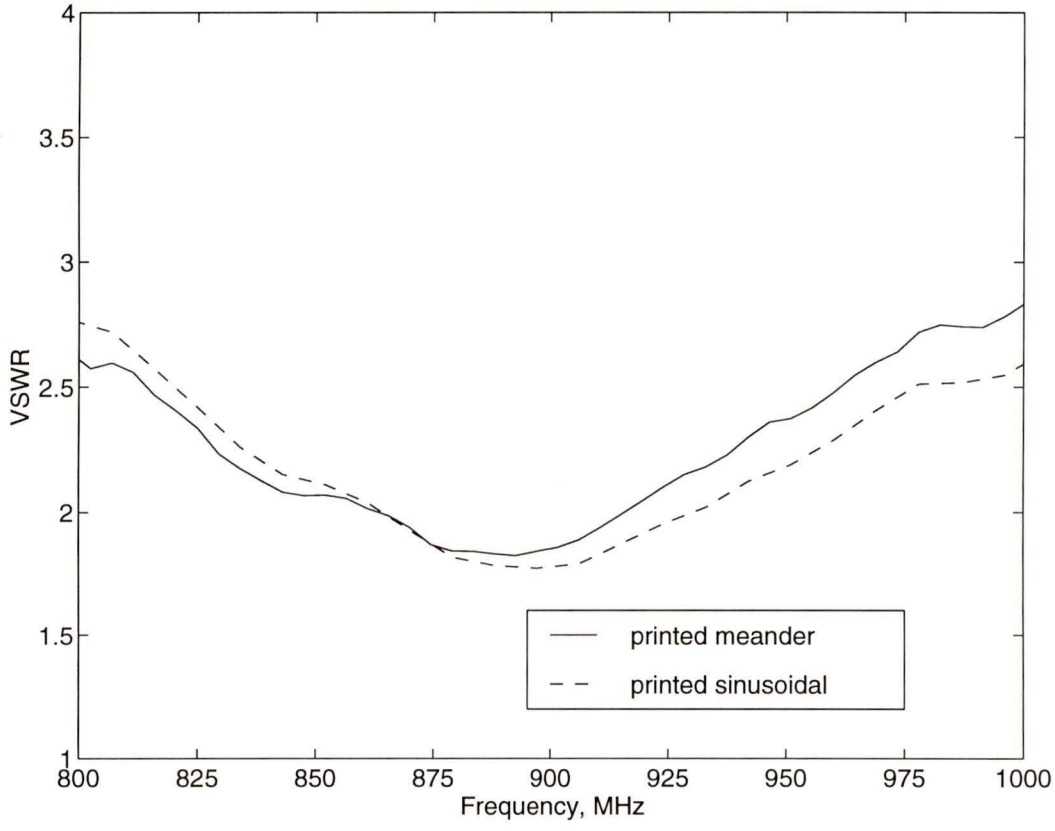

Figure 5.9: VSWR vs frequency characteristics of printed bent antennas

According to Fig. 5.9, once again like the wire sinusoidal antenna, the printed sinusoidal antenna has a better VSWR frequency response than the meander antenna for the same shortening ratio. The printed sinusoidal antenna has a bandwidth of 7.42% with a minimum VSWR of 1.77 in comparison to that of 6.02% and 1.83 of the meander. It may be mentioned that both the antennas are operating at a center frequency of 892.5 MHz.

5.2.2 Summary

A printed sinusoidal antenna has been developed that has a shortening ratio of 29.64% and a bandwidth of 7.42%. A printed meander antenna has also been developed with the same shortening ratio and a bandwidth of 6.02%.

5.3 Sleeve Antennas

5.3.1 Straight Sleeve Antenna

Several sleeve antenna configurations were investigated for broadband or dual band applications. Initially, a straight monopole antenna along with two matching posts as sleeves made from the same wire which was used for experimentation. The arrangement is shown in Fig. 5.10(a), where s is the sleeve spacing and L is the sleeve length. According to the design in section 3.3, a constant sleeve spacing of $2s = 3.2$ cm was used and the sleeves were initially made 7.0 cm long. During the

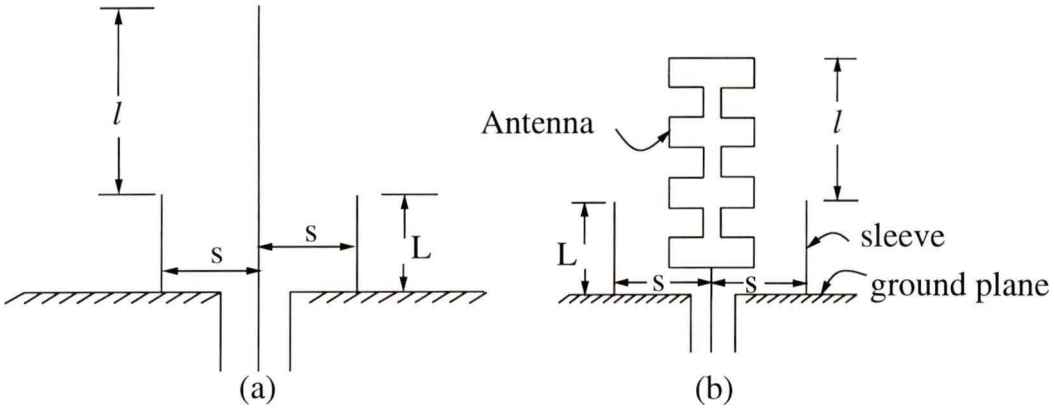

Figure 5.10: Sleeve antennas: (a) The straight sleeve antenna, and (b) the dual meander sleeve antenna

experiment those were trimmed and the VSWR response recorded.

The VSWR frequency response of the sleeve monopole antenna of Fig. 5.10(a) is shown in Fig. 5.11. The frequency range of operation was $700 - 2100$ MHz. The curves are plotted with the sleeve length as the parameter. Thus according to Fig. 5.11(a), the bandwidth of the sleeve antenna is $1.58 : 1$ within a VSWR $\leq 2 : 1$ when $L = 5.5$ cm. With further reduction in sleeve length the bandwidth of the antenna increases until $L < 3.4$ cm. For example with $L = 3.4$ cm the bandwidth of the antenna has been found to be $2.8 : 1$ with comparatively high values of VSWR (≤ 5).

In comparison to the straight quarter wave length monopole (marked by zero sleeve length in Fig. 5.11(a)), the straight sleeve antenna with $L = 3.4$ cm is a broadband antenna. This broadbanding technique will be used to accomplish our objective to develop a short antenna for application in both PCN bands.

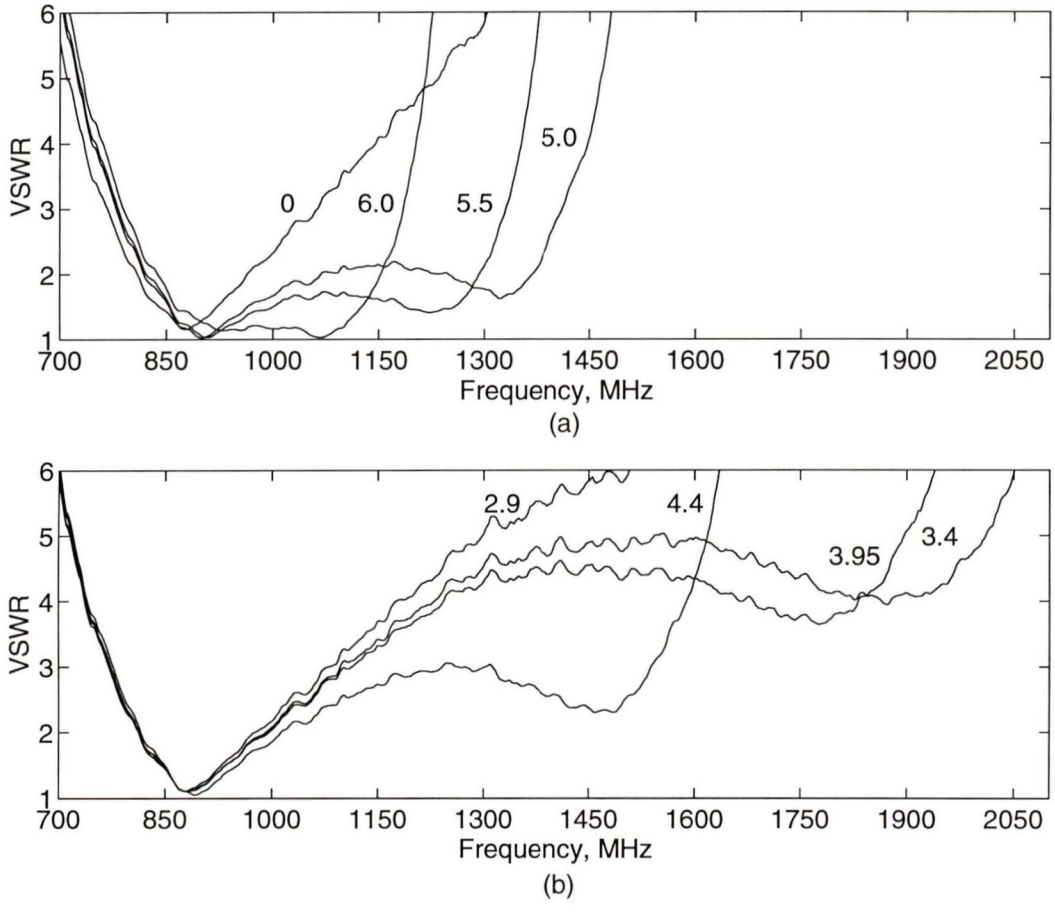

Figure 5.11: VSWR vs frequency characteristics of the straight sleeve antenna; sleeve length L (cm) is the parameter.

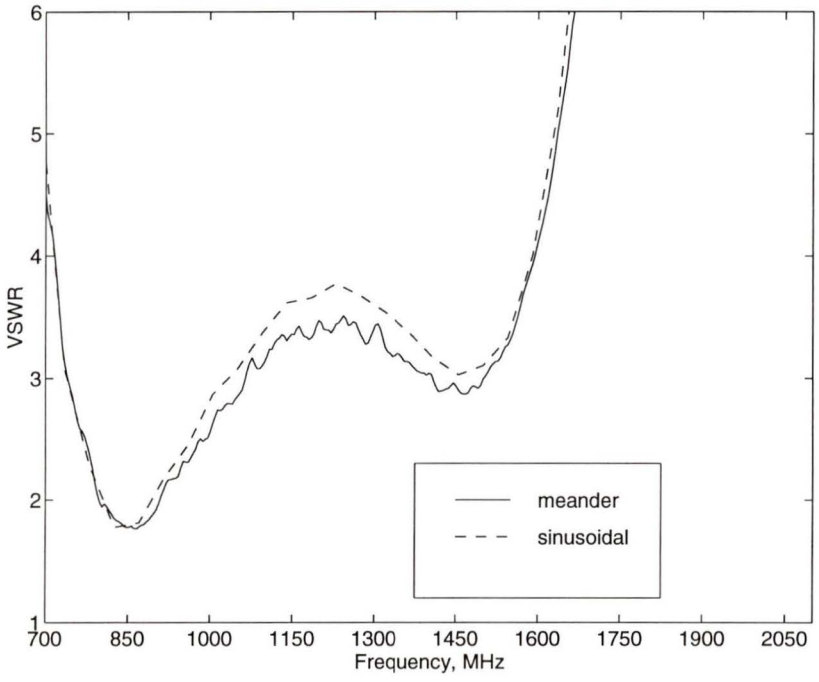

Figure 5.12: VSWR vs frequency characteristics of bent sleeve antennas

5.3.2 Bent Sleeve Antennas

The sleeve antennas investigated in this section are associated with the meander [Fig. 3.4(a)], the sinusoidal [Fig. 3.4(b)] and the dual meander [Fig. 3.6(b)] antennas. All three antennas were investigated when two posts were used as sleeves. Similar to the straight sleeve antenna, the sleeves were made from the same wire that was used to make the antennas. The procedure for the straight sleeve antenna was repeated here to determine the appropriate sleeve length.

The best VSWR frequency response that was found for the meander and the sinusoidal antenna is shown in Fig. 5.12. The dimensions of the meander and the sinusoidal antenna are listed in Table 5.1. The VSWR response of these two

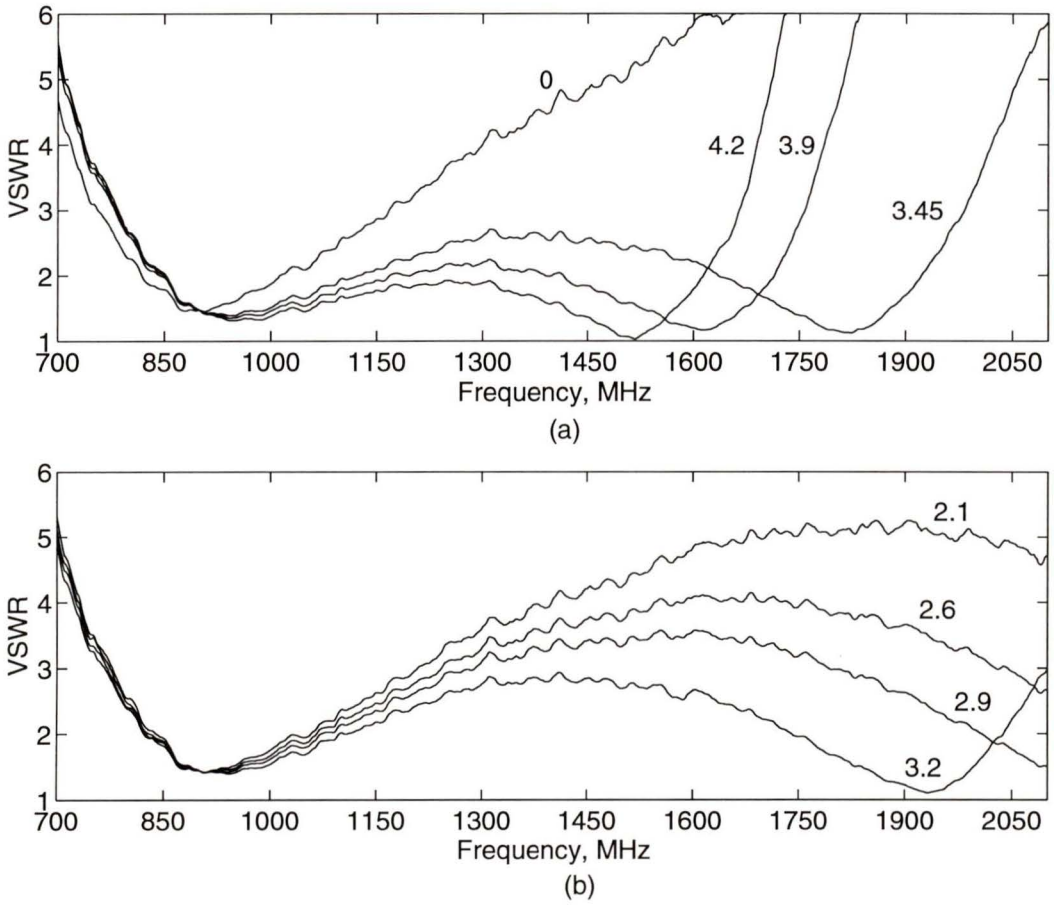

Figure 5.13: VSWR vs frequency characteristics of a dual meander sleeve antenna; sleeve length L (cm) is the parameter.

antennas with sleeves are found to be unsuitable for dual band operation.

Therefore, we considered a dual meander antenna [Fig. 3.6(b)] for this purpose following the work of Wong *et al.* [10] on it. The VSWR frequency response for the dual meander antenna with two posts as sleeves are shown in Fig. 5.13 with sleeve length as the parameter.

The results of our investigation show that the dual meander antenna when op-

erated with two matching posts as sleeves has a bandwidth of 1.89 : 1 with a sleeve length of 4.2 cm when VSWR $\leq$ 2 : 1. When the sleeve length is 3.2 cm, the antenna can operate in both the PCN bands (880 MHz and 1900 MHz). In the lower band this antenna has a bandwidth of 38.76% when the center frequency is 900 MHz. In the upper band (center frequency 1930 MHz) this antenna has a bandwidth of 14.43%. Also at the same time this antenna is 18% shorter than a straight quarter-wave monopole.

5.3.3 Summary

Keeping the spacing between the sleeves constant, straight sleeve antennas and dual meander antennas with sleeves were developed by varying the sleeve length. It has been found that a dual meander antenna with sleeves can operate over a frequency range of 1.89 : 1 within a VSWR of 2 : 1 when $L = 4.2$ cm. It has also been demonstrated that the same antenna with sleeve length $L = 3.2$ cm can be used in both the PCN bands.

Chapter 6

Discussion and Conclusions

6.1 Discussion

6.1.1 The Phenomenon of Shortening in Bent Antennas

It has been demonstrated in section 5.1.1 that the bent linear antennas resonate at a length less than a straight monopole. Defining this phenomenon as *early resonance*, a possible explanation of it can be given using concepts of electric circuits.

Let us consider the straight antenna of section 5.1.1 with resonant length of 0.233λ. The input impedance characteristics of this antenna is shown in Fig. 5.1 and 5.3. According to these characteristics the input impedance of any monopole antenna before resonance can be considered as a resistance and a capacitance connected in series. If an external inductance is connected in series at the input of

this antenna, it will add up with its input reactance and will move the reactance curve upwards meaning that the antenna will resonate at a length less than 0.233λ. The resonant antenna length will of course depend upon the value of the series inductance.

This process of tuning an antenna is very common in electrically small dipoles. Consider the example of the small dipole in section 1.1.1. The input capacitive reactance of the dipole (483.99 Ω) can be tuned by adding an inductance at the input. This will make the small dipole to resonate at a length of 0.24 λ. The main limitation in such a case, however, is associated with the value of the resonant resistance, R_{res} because as mentioned in section 1.1.1, when an antenna resonates at a shorter length, R_{res} drops to a low value resulting in high VSWR and low efficiency.

The phenomenon of *early resonance* in bent antennas can be explained using the above mentioned concept of tuning a short antenna by adding an inductance at the input. The task of adding inductance at the input is accomplished by bending antennas because as an antenna is bent, inductance is produced. The inductive reactance thus adds up with the capacitive reactance of the bent antenna and moves the reactance curve up thereby making it resonating at a shorter length. However, at present the process or model to separate the inductive and the capacitive reactances of a bent antenna are not known.

We know that the self inductance of a solenoid can be expressed as [42]

$$L = \mu_r \mu_o N^2 \frac{A}{l} \tag{6.1}$$

where $\mu_r = 1$ for air and $\mu_o = 4\pi \times 10^{-7}$ H/m; N is the number of loops, l is the

length of the solenoid and A is the cross-sectional area of each loop.

Considering the expression for inductance of a solenoid let us assume that the self inductance of a bent antenna is proportional to the cross-sectional area under each half period, inversely proportional to the antenna length and proportional to the square of the number of half periods [see Fig. 2.2]. Consider the three zigzag antennas of Nakano *et al.* [9], parameters of which are listed in Table 3.4.

The approximate self inductances of these antennas calculated using the above mentioned assumption are 0.00578μH, 0.01180μH, and 0.01545μH. Shortening ratios of these antennas as reported by Nakano and his colleagues [9] are 10, 24, and 34 percent. Therefore, by increasing the inductance the shortening ratio of the zigzag antenna is increased. Similarly, by changing the P/A ratio of the sinusoidal antennas we either increase or decrease the series inductance which makes the antenna more or less shorter.

6.1.2 Advantages and Limitations of The New Antennas

The Wire Sinusoidal Antenna

The only advantage of using a bent antenna is its reduced length. It is known from the work of Nakano *et al.* [9] that with increased shortening the radiation resistance of a zigzag antenna decreases [see Table 3.4]. It has also been predicted in section 3.2.1 that this reduction in radiation resistance will eventually make those antennas narrowband. However, the bandwidth characteristics of those antennas and its relationship with the design parameters [A and P in Fig. 2.2] have not been

investigated before.

Therefore, to understand the bandwidth behavior of such antennas we investigated a number of wire sinusoidal antennas which are similar to the zigzag. A parameter P/A has been defined for the sinusoidal configuration which can be correlated with both the shortening ratio and the bandwidth.

Consider the experimental results presented in Table 5.3, 5.4 and 5.5. It is clear from these results that with decreasing P/A, the shortening ratio increases. But this increase in shortening ratio is not without limitations. It is also clear that with decreasing P/A, the bandwidth becomes narrower. Therefore, the shortening ratio that can be achieved with these antennas is always limited by the required bandwidth. Depending upon different application requirements the shortening ratio will certainly be different. For example, if higher VSWR is not a problem in some receiving applications, then referring to Table 5.5 a shortening ratio of 44.71% can be achieved with a minimum VSWR of 2.95.

As a possible PCN handset antenna we suggest the sinusoidal antenna with a shortening ratio of 24.71% and a bandwidth of 5.26%. If still more shortening is intended with the same bandwidth, then impedance matching techniques should be used to lower the VSWR curve [see Fig. 5.5 and 5.6].

Another important point to note here is that the sinusoidal antenna has better VSWR frequency characteristics than the meander. Comparing the results for the sinusoidal antenna [Table 5.3, 5.4 and 5.5] with that of the meander antenna [Table 5.6], it is clear that the former is wideband and has lower minimum VSWR than the later for any shortening ratio. This is also demonstrated in Fig. 5.8.

The Printed Sinusoidal Antenna

According to the experimental results of Table 5.3, 5.4 and 5.5 we have predicted that the bandwidth of a sinusoidal antenna should be within 8.07%to 5.26% for P/A between 3.17 and 2.71. Therefore, an optimum P/A of 2.8 was selected to make a printed sinsusoidal antenna for a PCN handset. It has been found that the sinusoidal antenna with the above mentioned P/A ratio has a shortening ratio of 29.64% and a bandwidth of 7.42% when etched on fiberglass dielectric substrate ($\epsilon_r = 4.2$). This bandwidth should be adequate for a PCN handset [4].

To achieve larger shortening there are three specific suggestions:

1. Similar to the suggestion in wire sinusoidal antennas, the P/A ratio is to be decreased. But this will reduce the operational bandwidth of the antenna because the VSWR curve will move up. However, impedance matching techniques can be used to lower the VSWR curve and thereby increase the bandwidth of the antenna.

2. Yu *et al.* [4] proposed a printed meander antenna on a Duroid 6010 substrate ($\epsilon_r = 10.2$) with a shortening ratio of 34.1% and a bandwidth of 7.3%. Referring to their work the sinusoidal antenna here can be etched on a substrate like Duroid 6010 with higher dielectric constant which will certainly increase its shortening ratio still further beyond 29.64%. But it is also a fact that Duroid 6010 will be more expensive than fiberglass.

3. Similar to the work of Nakano *et al.* [35], [36], thicker substrates can be used. Nakano and his colleagues have used a substrate that has a thickness of 0.10λ.

It may be mentioned here that the substrate that has been used here has a thickness of 0.00446λ.

The Dual Meander Sleeve Antenna

A dual meander sleeve antenna has been developed that can be used as a dual band antenna in both the PCN bands (880 MHz and 1900 MHz). It can be seen from Fig. 5.11(a) that a straight monopole antenna cannot be used in both the PCN bands. Only properly designed sleeve antennas or other broadband antennas can be used in such applications.

A dual meander [see Fig. 3.6(b) and Table 3.5] antenna has been developed with properly selected sleeves of length 3.2 cm which can be operated as a dual band antenna. Referring to Fig. 5.13 this dual meander sleeve antenna can operate in both the PCN bands with more than adequate bandwidth (in the lower band 38.76% and in the upper band 14.43%). Also this antenna provides a shortening ratio of 18% in the lower band.

In the course of our experimental analysis it has been found that the dual meander sleeve antenna has a bandwidth of 1.89 : 1 when the sleeve length is 4.2 cm. It is indeed a broadband antenna which can be suggested for other applications. It is relevant to mention that the dual meander sleeve antenna of Wong *et al.* [10] has a bandwidth of 1.35 : 1.

Another advantage of this dual meander sleeve antenna ($L = 4.2$ cm in Fig. 5.10(b)) is that unlike other wideband antennas (that of Friedman [33], Bailey [32] and Dey *et al.* [34]), it has no complicated impedance matching or tuning arrange-

ments except the two sleeves. The only limitation is that the shortening ratio is not high (18%).

6.2 Conclusions

To implement the objective of developing small wideband antennas for application in PCN handsets the input impedance and the bandwidth characteristics of several bent antenna configurations have been investigated experimentally. The configurations considered for this purpose were - the meander, the sinusoidal, and the dual meander.

Three new antennas have been proposed for the above mentioned specific application requirement: the first one is a wire sinusoidal antenna with a shortening ratio of 24.71% and a bandwidth of 5.26%, the second one is a printed sinusoidal antenna on fiberglass substrate with a shortening ratio of 29.64% and a bandwidth of 7.42%, and the third one is a dual meander sleeve antenna with a shortening ratio of 18% which can be applied in both the PCN bands. Also another broadband dual meander sleeve antenna has been developed which has a bandwidth of 1.89 : 1 and has been suggested for some other applications.

The results for the wire sinusoidal antenna can be a guideline to any designer who is interested in a specific shortening ratio but is uncertain about its bandwidth limitations. It has been suggested that wherever more shortening is needed, impedance matching networks be designed for that specific antenna and implemented to lower the VSWR curve so that some operating bandwidth can be obtained. Another way

to achieve higher shortening can be to etch the configuration on substrates with higher dielectric constants or to use thicker substrates.

In the course of this work a possible explanation of the phenomenon of shortening in bent antennas has been presented. Future work is needed to verify the validity of this proposition. It has been demonstrated that the sinusoidal antenna has better VSWR frequency response than the meander when the shortening ratios of both the antennas are the same.

Although it has been predicted that characteristics like radiation pattern, polarization etc. of the bent antennas will be more or less similar to the straight monopole within the implemented design constraints, but it is recommended that those characteristics be investigated for the individual antenna considered for any specific application requirement.

Bibliography

[1] T. S. Rappaport, "Wireless Personal Communications: Trends and Challenges," IEEE Antennas Propagat. Magazine, Vol. 33, No. 5, Oct. 1991, pp. 19-29.

[2] D. C. Cox, "Personal Communications — A Viewpoint," IEEE Communications Magazine, Nov. 1990, pp. 8-20.

[3] R. Steele, "Deploying Personal Communication Networks," IEEE Communications Magazine, Sept. 1990, pp. 12-15.

[4] C. Yu and K. Ju, "Printed circuit dipole antenna for personal communication network handset," Microwave and Optical Technology Letters, vol. 5, no. 10, Sept. 1992, pp. 477-480.

[5] H. H. Xia, H. L. Bertoni, L. R. Maciel, A. L. Stewart, and R. Rowe,"Radio propagation characteristics for line-of-sight microcellular and personal communications," IEEE Trans. Antennas Propagat. vol. 41, no. 10, Oct. 1993, pp. 1439-1446.

[6] H. A. Wheeler, "Small Antennas," IEEE Trans. Antennas Propagat., vol. AP-23, no. 4, July 1975, pp. 462-469.

[7] C. A. Balanis, *Antenna Theory Analysis and Design*, Harper and Row Publishers, NY, 1982. pp. 105, 443, 333, 332-337, 118, 118, 115, 119, 20, 53, 127, 120-124, 290-295, 44-45, 58, 48-53, 333.

[8] W. L. Stutzman, G. A. Thiele, *Antenna Theory and Design*, John Wiley and Sons, Inc., USA, 1981. pp. 101-104, 260, 202, 278, 279, 279, 202, 202.

[9] H. Nakano, H. Tagami, A. Yoshizawa, and J. Yamauchi, "Shortening ratios of modified dipole antennas, " IEEE Trans. Antennas Propagat., vol. AP-32, no.4, April 1984, pp. 385-386.

[10] J. L. Wong, H. E. King, "Height reduced meander zigzag monopoles with broadband characteristics," IEEE Trans. Antennas Propagat., vol. AP-34, no. 5, May 1986, pp. 716-717.

[11] J. Rashed, and C. T. Tai, "A new class of resonant antennas," IEEE Trans. Antennas Propagat., vol. AP-39, no. 9, Sept. 1991. pp. 1428-1430.

[12] J. Rashed-Mohassel "The radiation characteristics of a resonant meander line section as a monopole," Microwave and Optical Technology Letters/vol. 4, No. 12, Nov. 1991. pp. 537-540,

[13] R. W. P. King, *The Theory of Linear Antennas*, Harvard University Press, Cambridge, MA, 1956.

[14] R. S. Elliott, *Antenna Theory and Design*, Englewood Cliffs, N.J. : Prentice Hall, 1981. pp. 277-321, 297, 300-301, 301, 302.

[15] R. F. Harrington, *Field Computation by Moment Methods*, IEEE Press, NY, 1993.

[16] M. N. O. Sadiku, *Numerical Techniques in Electromagnetics*, CRC Press, USA, 1992.

[17] J. J. H. Wang, *Generalized Moment Methods in Electromagnetics*, John Wiley and Sons, Inc. , USA, 1991.

[18] F. M. Landstorfer and R. R. Sacher, *Optimisation of Wire Antennas*, Research Studies Press Ltd. Letchworth, Hertfordshire, England, 1985.

[19] J. H. Richmond, "Monopole antenna on a circular disk," IEEE Trans. Antennas Propagat., vol. AP–32, no. 12, Dec. 1984. pp. 1282-1287.

[20] Awadalla K. H., and Maclean T. S. M., "Monopole antenna at the center of a circular ground plane: input impedance and radiation pattern," IEEE Trans. Antennas Propagat., vol. Ap-27, Mar.1979. pp. 151-153.

[21] H. M. Ibrahim, "Radiation pattern of a $\frac{\lambda}{4}$ monopole mounted on a small thick circular disk," Journal Electronics, 1990, vol. 68, no. 2, pp. 283-292.

[22] S. Bhat, "The input impedance of a monopole antenna mounted on a cubical conducting box," IEEE Trans. Antennas Propagat., vol. AP-35, no. 7, July. 1987. pp. 756-762.

[23] A. W. C. Chu, S. A. Long and D. R. Wilton, "The radiation pattern of a monopole antenna attached to a conducting box," IEEE Trans. Antennas Propagat., vol. 38, no. 12, Dec. 1990. pp. 1907-1911.

[24] J. Toftgard, S. N. Hornsleth, and J. B. Andersen, "Effects on portable antennas of the presence of a person," IEEE Trans. Antennas Propagat., vol. 41, no. 6, June 1993. pp. 739-746.

[25] M. M. Weiner, S. P. Cruze, C. Li, W. J. Wilson, *Monopole Elements on circular Ground Planes*, Artech House, Norwood , MA, 1987. pp. 4, 3, 62-64, 68.

[26] B. Josephson, "The quarter wave dipole," IRE Wescon Conv. Rec., Part I, San Francisco, August 1957, pp. 77-90.

[27] R. King, "Asymmetrically driven antennas and the sleeve dipole," Proceedings of the IRE, Oct. 1950, pp. 1154-1164.

[28] R. A. Burberry, "Progress in aircraft aerials," The Proceedings of the Institution of Electrical Engineers, vol. 109, part B, no. 48, Nov. 1962. pp. 431-454.

[29] A. J. Poggio, P. E. Mayers, "Pattern Bandwidth optimization of the sleeve monopole antenna," IEEE Trans. Antennas Propagat., vol. AP-14, Sept. 1966. pp. 643-645.

[30] W. L. Weeks, *Antenna Engineering*, McGraw Hill, NY, 1968. pp. 322-323.

[31] H. E. King, and J. L. Wong, "An experimental study of a balun-fed open-sleeve dipole in front of a metallic reflector," IEEE Trans. Antennas Propagat., vol. AP-20, Mar. 1972. pp. 201-204.

[32] M. C. Bailey, "Broad–band half wave dipole," IEEE Trans. Antennas Propagat., vol. AP-32, no. 4, April. 1984, pp. 410-412.

[33] C. H. Friedman, "Wide–band matching of a disk loaded monopole," IEEE Trans. Antennas Propagat., vol. AP-33, no. 10, Oct. 1985, pp. 1142-1148.

[34] S. Dey, C. K. Anandan, K. A. Jose, P. Monahon, and K. G. Nair,"Wide–band printed dipole antenna," Microwave and Optical Technology Letters/vol. 4, No. 10, Sept. 1991. pp. 417-419.

[35] H. Nakano, S. R. Kerner, N.G.Alexopoulos, "The moment method solution for printed wire antennas of arbitrary configuration," IEEE Trans. Antennas Propagat., vol. 36, no. 12, Dec. 1988. pp. 1667-1673.

[36] H. Nakano, K. Hirose, T. Suzuki, S. R. Kerner, N.G.Alexopoulos, "Numerical analysis of printed wire antennas," IEE Proceedings, vol. 136, pt. H, No. 2, April 1989, pp. 98-104.

[37] K. K. Mei, "On the integral equations of thin wire antennas," IEEE Trans. Antennas Propagat., vol. AP-13, May 1965. pp. 374-378.

[38] R. C. Johnson, and H. Jasik, *Antenna Engineering Handbook*, Second Edition, McGraw–Hill Book Company, USA, 1984.pp. 4-4 to 4-5, 42-13.

[39] A. W. Rudge, *The Handbook of Antenna Design*, Peter Peregrinus Ltd. on behalf of the Institution of Electrical Engineers, 1986. pp. 1421-23, 1430.

[40] J. D. Kraus, *Antennas*, McGraw–Hill Book Company, USA, 1950. p. 535.

[41] H. Nakano, J. Yamauchi, K. Kawashima, and K. Hirose, "Effects of arm bend and asymmetric feeding on dipole antennae," Int. J. Electronics, 1983, vol. 55, no. 3, pp. 353-364.

[42] D. A. Bell, *Fundamentals of Electric Circuits*, Fourth Edition, Prentice Hall, NJ, 1988. P. 351.

VITA

Surname: Ali | Given Names: Mohammod

Place of Birth: Kushtia, Bangladesh | Date of Birth: January 16, 1963

Educational Institutions Attended:

Bangladesh University of Engineering and Technology, Dhaka	1982 to 1987
University of Victoria	1992 to 1994

Degrees Awarded:

B. Sc Eng. (Electrical & Electronic)
Bangladesh University of Engineering & Technology, Dhaka 1987

PARTIAL COPYRIGHT LICENSE

I hereby grant the right to lend my thesis to users of the University of Victoria Library, and to make single copies only for such users or in response to a request from the Library of any other university, or similar institution, on its behalf or for one of its users. I further agree that permission for extensive copying of this thesis for scholarly purposes may be granted by me or a member of the University designated by me. It is understood that copying of this thesis for financial gain shall not be allowed without my written permission.

Title of Thesis :

Small Linear Antennas

Author: [redacted]

Mohammod Ali

August 15, 1994